
# $Ru_xBi_{1-x}$-oxide electrodes for electrochemical pseudo-capacitors

Written by: Hao Yu (260783760)

April 2019

A thesis submitted to McGill University in partial fulfillment of the requirements of the degree of M.Eng

Department of Chemical Engineering, McGill University

Montréal, Québec, Canada H3A0C5

# Abstract

The global economy and environment have been influenced remarkably by the excessive use of non-renewable fossil fuels. Currently, we are undergoing a period that is shifting from relying on carbon-intensive sources of energy (oil, gas, coal) to green energy such as wind and solar in the form of electricity. Therefore, the demand and the market for energy storage devices of various applications has been increasing rapidly during the last few years [1].

Batteries, as (surplus) energy-storage devices, are currently favored by the market because they have large energy density and can provide suitable levels of power output for various applications. However, with the increasing demand for power/performance of more complex electronic and other devices, the disadvantages such as short lifetime and relatively low power density limited their applications. To solve this problem, a promising solution is to combine batteries with supercapacitors to create hybrid power sources. Currently, supercapacitor electrodes are mainly based on carbon materials and store energy by electrostatic charging of the electrochemical double-layer, which limits their energy density. Thus, much of research has been focused on developing new electrode materials that can store a larger amount of energy, i.e. on developing pseudocapacitors based on the use of MMO (Mixed Metal Oxides) electrodes that can yield higher energy and power density due to the occurrence of fast and reversible redox reactions in the solid phase [2].

In this work, thermally-prepared $Ru_xBi_{1-x}$-oxide coatings of various composition were formed on a Ti substrate, with the aim of investigating the influence of Bi-oxide addition on the resulting charge storage/delivery capacity of the oxide. Electrochemical tests (cyclic voltammetry, galvanostatic charge/discharge, and electrochemical impedance spectroscopy) were performed on the coatings in a three-electrode cell at 295 K and under atmospheric pressure, while galvanostatic charge/discharge experiments were also performed in a two-electrode cell. In addition, the surface topography and morphology of $Ru_xBi_{1-x}$-oxide coatings and distribution of elements were investigated by SEM/EDS.

It was found that addition of Bi-oxide into the Ru-oxide coating resulted in a significant change in the oxide's charge storage/delivery capacity, yielding a bell-shaped dependence with a maximum value offered by the $Ru_{0.6}Bi_{0.4}$-oxide coating ($195 \pm 11$ mF/cm$^2$), which is significantly higher than the current state-of-the-art electrode material based on two-dimensional electrodes, pure

ruthenium oxide. In the two-electrode configuration, the material yielded even a higher capacitance ($266 \pm 51$ mF/cm$^2$ at 3 mA/cm$^2$), making this material a promising candidate as a pseudocapacitor electrode material.

# Résumé

L’utilisation excessive de combustibles fossiles non renouvelables a eu une influence considérable sur l’économie et l’environnement au niveau mondial. Actuellement, nous sommes en train de passer d'une source d'énergie à base de carbone (pétrole, gaz, charbon) à une énergie verte telle que le vent et le soleil sous forme d'électricité. Par conséquent, la demande et le marché des dispositifs de stockage d'énergie d'applications diverses ont augmenté rapidement au cours des dernières années [1].

Les batteries, en tant que dispositifs de stockage d'énergie, sont actuellement privilégiées par le marché car elles ont une densité d'énergie élevée et peuvent fournir des niveaux de puissance de sortie appropriés pour diverses applications. Cependant, face à la demande croissante de performances d'appareils plus complexes, des inconvénients tels qu'une durée de vie réduite et une densité de puissance relativement faible ont limité leurs applications. Pour résoudre ce problème, une solution prometteuse consiste à combiner des batteries avec des supercondensateurs pour créer des sources d'alimentation hybrides. Actuellement, les électrodes de supercondensateurs sont principalement basées sur des matériaux à base de carbone et stockent de l'énergie par chargement électrostatique de la double couche électrochimique, ce qui limite leur densité d'énergie. Ainsi, de nombreuses recherches ont été consacrées au développement de nouveaux matériaux pour électrodes pouvant stocker une plus grande quantité d’énergie, notamment au développement de pseudo condensateurs basés sur l’utilisation d’électrodes MMO (Oxydes Métalliques Mixtes) pouvant générer une énergie et une densité de puissance plus élevées du fait de l’apparition de réactions redox rapides et réversibles en phase solide [2].

Dans ce travail, des revêtements de $Ru_xBi_{1-x}$-oxyde de différentes compositions préparés thermiquement ont été formés sur un substrat de Ti, dans le but d'étudier l'influence de l'addition de d’oxyde de Bi sur la capacité résultante de stockage/libération de charges de l'oxyde. Des tests électrochimiques (voltamètrie cyclique, charge/décharge galvanostatique et spectroscopie d'impédance électrochimique) ont été effectués sur les revêtements dans une cellule à trois électrodes à 295 K et sous pression atmosphérique, tandis que des expériences de charge/décharge galvanostatiques ont également été réalisées dans une cellule à deux électrodes. De plus, la topographie de surface et la morphologie des revêtements $Ru_xBi_{1-x}$-oxyde et la distribution des éléments ont été étudiées par SEM/EDS.

Il a été constaté que l'ajout d'oxyde de Bi dans le revêtement d'oxyde de Ru entraînait un changement significatif de la capacité de stocker/délivrer les charges de l'oxyde, produisant une dépendance en forme de cloche avec une valeur maximale offerte par le revêtement d'oxyde de $Ru_{0.6}Bi_{0.4}$ (195 ± 11 mF/cm$^2$), ce qui est considérablement plus élevé que le matériau d'électrode de pointe actuel, à savoir l'oxyde de ruthénium pur. Dans la configuration à deux électrodes, le matériau permettait d'obtenir une capacité encore plus élevée (266 ± 51 mF/cm$^2$ à 3 mA/cm$^2$), ce qui en faisait un candidat prometteur en tant que matériau d'électrode pseudo-condensateur.

# Acknowledgment

I would like first to thank my supervisor Prof. Sasha Omanovic for providing me this valuable opportunity to finish my master's study and offering guidance on my project throughout the process. Your friendly attitude toward students and collogues makes me feel relaxed and full of energy to conduct research. Your professional expertise has always steered me in the right directions and allowed me to be independent for my future research. Thank you for your kind encouragement and suggestions whenever I need help during the last two years.

I would also like to say thank you to my officemate Aqeel. Thanks for giving me suggestions and offering help for every aspect of my life from the first day I came to the office. Thanks for helping me fitting into this new environment when I first came. Your encouragement and help mean a lot to me. Thank you, my friend Deepak, for teaching me basic electrochemical knowledge and techniques from the first day I worked in our Electrochemical and Corrosion lab. Your help enabled me to work more efficiently on my project. I wish you two the best of luck and I am sure huge success is waiting for you ahead. Maybe we will meet each other in some other places in the world.

Thank you, my friends and colleagues. Xingge, Zhuoya, Elmira, Jeff, Rihab, Emmanuel, Abraham and Mike, I appreciate all your kindness help, suggestions on my research, valuable lab skills, as well as funny jokes we shared together. I wish you all good luck for your future endeavours and I have no doubt that you will be successful on whatever you do.

Finally, I must express my gratitude to my parents and to my grandparents. Your endless support and continuous encouragement throughout my years of study are the most valuable for me. This work would not have been possible without them. Thank you.

# Contents

# List of Figures

# List of Tables



# List of Equations

# Chapter 1: Introduction

With most of the world's energy supply coming from fossil fuels (57.67%) [3], some parts of the world are already suffering from severe environmental problems such as water/air pollution and extreme weathers caused by climate change. Therefore, a great deal of effort has been made to explore efficient, clean and sustainable energy resources, as well as novel technologies regarding energy storage, conversion, and utilization. Among different technologies for energy storage and utilization such as fuel cells, batteries and supercapacitors, electrochemical capacitors have gained much attention due to their high power density, short charging/discharging time and long lifecycle. Because of these advantages, supercapacitors have a broad range of applications, including hybrid electric vehicles and trams [4, 5], military equipment, street lights, cameras and phones, as well as in the field of aviation [6].

Various carbon-based materials have been intensely studied for use as material for supercapacitor electrodes, such as activated carbon [7], CNTs [8], carbon nanofibers [9], graphite [10] and carbon aerogels [11]. Some advantages of these materials are non-toxicity, low cost, easily accessible, posses high chemical stability, and can operate in a wide operating temperature range [12]. However, supercapacitors that are based on electrical double-layer charging using carbon materials tend to have lower specific capacitance and energy density, which limit their usage in many aspects.

To address this problem, a promising solution is to use transition metal oxides as pseudocapacitance materials to produce supercapacitors, which can have fast and reversible faradic redox reactions on the surface of the electrodes and within the thin sub-surface region. For example, hydrous $RuO_2$ is recognized as the most efficient and promising supercapacitor electrode material due to its high specific capacitance, high conductivity, good electrochemical reversibility and stability. However, the commercial production of ruthenium oxides for electrodes has been hampered predominantly by its high costs (currently about more than 2000 USD/kg [13]). Therefore, investigation toward other inexpensive or mixed metal oxides is considered a promising field of study.

Batteries, on the other hand, are known as the most commonly used energy storage devices and are favored by the market for their higher energy density (relative to capacitors). But with the increasing demand for power performance of more complex electronic devices, the drawbacks of batteries such as short life-time, low power density and long charging-discharging time limited their

future use to a great extent. The detailed comparison between (super)capacitors and batteries in terms of their specific power and energy is shown in Figure 1 below [14, 15]. The ultimate aim of research on supercapacitors is to maintain their high specific power, while at the same time improving their specific energy.

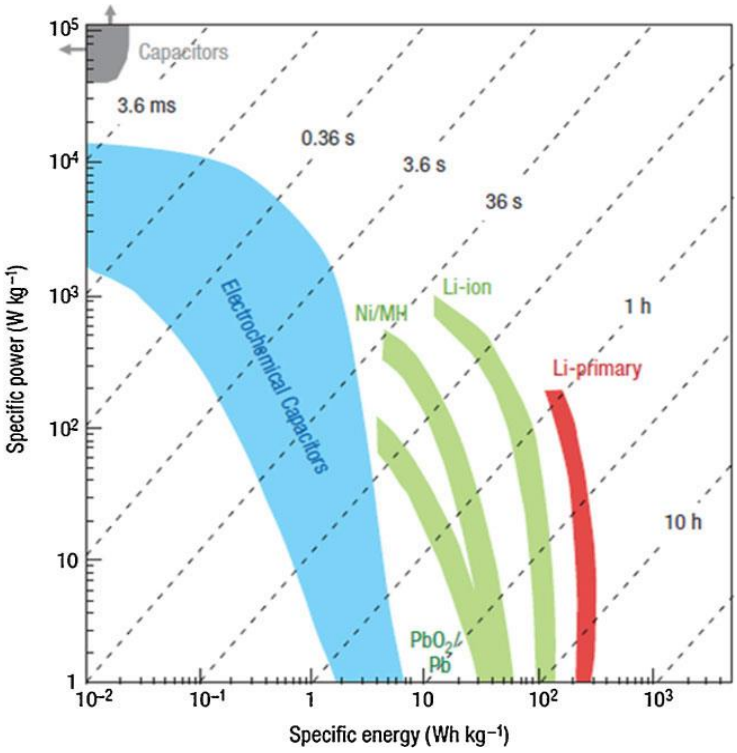


Figure 1 Ragone plot of current energy storage and conversion devices [15].

Instead of viewing batteries and supercapacitors as competing technologies, it is more beneficial to view their relationship as complementing. The future technology that combines batteries and supercapacitors together to create hybrid energy storage and utilization system might be the answer to utilize electricity in a more efficient manner. However, limited by the electrode materials, current supercapacitors are not able to achieve desired energy density. To compensate for this disadvantage, pseudocapacitors are being considered to solve the problem.

The goal of this research is to contribute to the development of new electrode materials for pseudocapacitors by combining inexpensive bismuth oxide ($Bi_2O_3$) with high-performance ruthenium oxides ($RuO_2$) to produce binary oxide material $Ru_xBi_{1-x}O$ ($0 \leq x \leq 1$). The aim is to lower the costs

of electrodes materials and meanwhile maintain or even improve the capacitance behavior of the oxide coatings.

# Chapter 2: Background

## 2.1 Supercapacitors

According to the charge-storage mechanisms, supercapacitors (SC) can be classified into three categories: electric double-layer capacitors (EDLC), pseudocapacitors and hybrid capacitors, as shown in Figure 2.

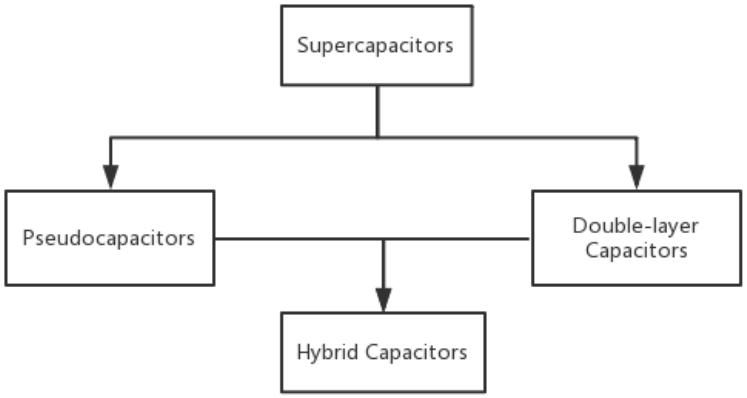


Figure 2 Diagram that shows the classification of supercapacitors.

### 2.1.1 Electric Double-layer Capacitors

A typical EDLC consists of two electrodes, electrolyte and a separator. The electrodes are normally porous carbon materials with large surface area, such as activated carbon, CNTs, or carbon black. The separator membrane is to prevent the two electrodes from direct contact (short-circuiting).

In a double-layer capacitor, the charges are stored within the Helmholtz double layer that exists between the surface of electrodes and electrolyte. A very simplified schematic of the electric double-layer is shown in Figure 3 [16]. Since there is no charge transfer across the interface, this mechanism is a pure capacitance effect, i.e. electrostatic charging.

During the charging process, electric double-layers appear on both electrodes when a voltage is applied to an EDLC. The positively charged or negatively charged electrodes are balanced by the accumulation of counter-ions from the bulk of the electrolyte to achieve electroneutrality. In this process, no chemical reaction is involved, which gives EDLCs superior charging and discharging stability, long life-span and very fast recharging time.

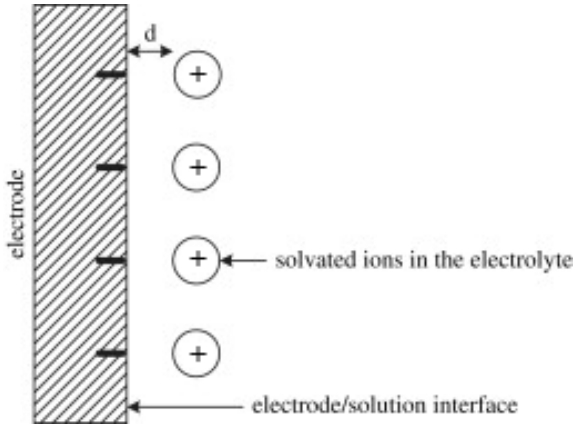


Figure 3 A simplified schematic of electric double-layer [16].

The capacitance (F) of an EDLC can be estimated by the equation:

$$C = \frac{\varepsilon_0 \cdot \varepsilon_r \cdot S}{d} \qquad \text{Equation 1}$$

$\varepsilon_r$ is the value of relative dielectric constant, $\varepsilon_0$ is the vacuum permittivity equals to approximately $8.85 \times 10^{-12}$ farad per meter (F/m), $d$ is the thickness of the electric double-layer (m), and $S$ is the surface area of the electrode ("plate") ($m^2$) [17]. A smooth electrode in concentrated electrolyte solution can have a capacitance of 10-30 $\mu F/cm^2$ [16].

### 2.1.2 Pseudocapacitors

In a pseudocapacitor, electrical energy is stored by electron charge transfer between electrode and electrolyte, through electrosorption, reduction-oxidation reactions and intercalation processes [18, 19]. Unlike EDLCs where energy is stored electrostatically with no reactions between the electrodes and the ions, pseudocapacitors store charges through fast and highly reversible redox reactions. This

is the main reason that pseudocapacitors can normally have much larger capacitance comparing with EDLCs [16].

Many transition metal oxides such as ruthenium oxides, iridium oxides, iron oxides and manganese oxides can have faradaic electron-transferring reactions with low conducting resistance [20].

For example, the electron transfer reactions of transition metal oxides can be expressed as [21]:

$$MO_a(OH)_b + \mathrm{x}H^+ + xe^- \rightleftharpoons MO_{a-x}(OH)_{b+x}$$

where $MO_a(OH)_b$ and $MO_{a-x}(OH)_{b+x}$ indicate interfacial $MO_a \cdot nH_2O$ in higher and lower oxidation states, respectively. Thus, the charge storage/discharge is based on the reversible and fast transition of M between two oxidative states, in which the charge of the metal is compensated by intercalation of $H^+$ in the solid phase.

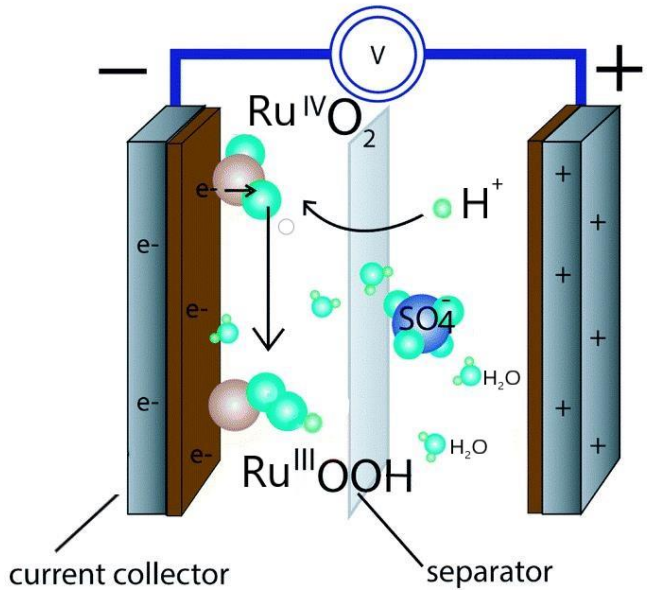


Figure 4 Pseudocapacitance material $RuO_2$ storing charges through Faradaic reaction [14].

Figure 4 above is the diagrammatic drawing of the pseudo-capacitance material $RuO_2$ storing charges through Faradaic reactions. During the charging and discharging process, protons ($H^+$) are

incorporated into or removed from the $RuO_2$ crystal lattice. In this process, there is a change of Ru-oxide between the two forms, $RuO_2$ and RuOOH, with the involvement of $H^+$ ions. This reaction occurs within the top-most layer of the Ru-oxide.

It is worth to mention that different from redox reactions in batteries, the reactions in pseudocapacitors do not involve forming or breaking chemical bonds. For this reason, pseudocapacitors can charge and discharge within a short period of time and are more stable over time. The pseudocapacitance usually depends on various factors such as surface area, electrode material, and structure of the electrodes. With the same electrode surface area, the capacitance of a pseudocapacitor may be larger than that one of EDLC by a factor of 100 [15].

## 2.2 Literature Review

Currently, both EDLC and pseudocapacitance materials have been widely studied. The most widely used materials for EDLC electrodes are carbon-based materials such as graphene, activated carbon (AC), carbon nanotubes (CNTs), carbon nanofibers (CNFs) and activated carbon fabrics. The theoretical capacitance of graphene is the highest value reported, which is approximately 520 F/g. However, the experimental capacitance value achieved was only 39% of the theoretical value, yielding results from 135 F/g to 205 F/g [22, 23]. Besides, conducting polymers combined with graphene sheets have also been studied. Research of electrodes fabricated from polyaniline nanotubes (PANi-NT), polypyrrole (PPy) and graphene oxide (GO) have achieved a volumetric capacitance of 369.5 $F/cm^2$ [24].

Various transition metal oxides have been studied for use in pseudocapacitor materials, such as $MnO_2$, $RuO_2$, $FeO_x$, $CoO_x$, $NiO_x$, as well as some other materials [25]. All the materials showed great potential for practical use for pseudocapacitors. One research that utilized ultrathin films of $MnO_2$ deposited on multiwall carbon nanotubes (MWNT) has achieved a capacitance of 940 F/g [26], which is close to the theoretical capacitance of $MnO_2$ of 1370 F/g [27]. Another low-cost and environmentally friendly material, $FeO_x$, has also exhibited great potential for pseudocapacitance electrodes. The highly porous surface of $Fe_3O_4$ with an average crystallite size of 12 nm was found to have a specific capacitance of 740 F/g in 1 M $H_2SO_4$ electrolyte solution [28]. Ruthenium oxides have the largest theoretical capacitance (2200 F/g) [27] comparing to other metal oxides. Among the

research conducted, the experimental capacitance values fall in the range from 700 to 1700 F/g [29-32]. To further increase the capacitance of materials based on Ru-oxides, porous surface structures are normally used to increase the accessibility of the inner layer of metal oxides coatings.

Nonetheless, the high costs and toxic properties of ruthenium oxides prevented this promising material from widespread usage. Research has also been focusing on mixed metal oxides (MMO) due to their potential of high power and energy density for use in supercapacitor electrodes [33]. For example, a research on layered double hydroxides (LDHs) of Ni and Mn for pseudocapacitance materials has achieved a high capacitance value of 1881 F/g, which is higher than both Ni and Mn hydroxide alone [34]. However, some of the disadvantages of MMOs are the loss of catalytic activity, poor stability of the oxides coating layers, limited operation conditions, and electrolytic media resistance [35-39].

Currently, much research on mixing other metal oxides with ruthenium oxides has been conducted and showed promising potential for pseudocapacitors application. For example, a binder-free $Ir_{0.4}Ru_{0.6}$-oxide/functionalized multi-walled carbon electrode was fabricated and achieved 664 ± 7 F/g with excellent stability [40]. Besides, hydrous $30RuO_2$-$70SnO_2$ composites produced by a two-step hydrothermal process was found to have a capacitance of 1150 F/g and excellent capacitive characteristics [41].

To the best of our knowledge, no research has been focused on combining bismuth oxides with hydrous $RuO_2$ to produce electrodes for pseudocapacitors. Since bismuth oxides have excellent electrochemical properties, are of low costs and environmentally friendly, and can be oxidized in the solid phase, they are considered as good candidates for fabricating electronic devices [42]. Herein we report for the first time the method to produce $Ru_xBi_{1-x}$-oxide ($0 \leq x \leq 1$) composites, aiming to fabricate supercapacitor electrodes with better electrochemical performance while potentially reducing their cost relative to pure $RuO_2$. It should be noted that this particular work focused on providing initial data on the influence of Bi-oxide addition into the $RuO_2$ structure on the resulting charge storage properties, without further optimization of the material in terms of its structure/morphology in order to produce nano-structured electrodes for practical applications; this will be done in the future, with the best-performing composition identified in this work.

## 2.3 Market and Application

Supercapacitors have a broad range of real-life applications, including the area of hybrid vehicles, smartphones, military, and energy harvesting [43].

For example, supercapacitors are being used to increase the efficiency and reduce energy consumption for electric vehicles in several ways. Currently, the electric vehicles briefly turn off their engines when coming to a stop, and then start it again efficiently using the power stored in the supercapacitors. Supercapacitors can also be used to recover braking energy. It is estimated that there are over 600 thousand HEVs (hybrid electric vehicles) that use supercapacitors in their start-stop systems [44]. Branded as i-eloop, this application is claimed to reduce fuel consumption by approximately 10%.

With extended functional life-span, the demand for supercapacitors for storing renewable energy has increased significantly. In the solar energy and wind energy system, supercapacitors are frequently used to integrate with batteries to boost the power density of the overall system. Moreover, the use of supercapacitors can be found on consumer electronics, such as laptops, portable media players, LED flashlights in digital cameras and phones, as well as cordless electric screwdrivers.

As of 2016, the reported worldwide sales of supercapacitors are about US$400 million. Some of the major global supercapacitor manufacturing companies are Maxwell Technologies (U.S.), Nippon Chemi-Con Corp. (Japan), Panasonic Corporation (Japan), LS Mtron (South Korea), and Nessacap Co. Ltd (Canada).

According to IDTechEx, the global supercapacitor market is anticipated to account for $2 billion by 2026, with an annual increase of about 24%.

# Chapter 3: Experimental Procedures and Methods

## 3.1 Chemicals and Reagents

Electrochemical properties of binary metal oxides coatings of Ru/Bi-oxide for electrodes were studies in a standard three-electrode electrochemical cell employing 1 mol/L KOH (Fisher Scientific 1310-58-3) solution. 6 mol/L KOH was used as electrolyte in the two-compartment electrochemical coin-cell for galvanic charge/discharge and electrochemical impedance spectroscopy (EIS) tests. 0.15 mol/L metal precursor solutions for producing R/Bi-oxide coatings was prepared by dissolving $RuCl_3 \cdot xH_2O$ (Sigma Aldrich 206229) and $BiCl_3 \cdot 3H_2O$ (Acros Organics 7787-60-2) salts into 50% iso-propanol (purity 99.9%, Fisher Scientific A416-1) and 50% hydrochloric acid (37wt.% Fisher Scientific 7647-01-0) mixture. All aqueous solutions were prepared using deionized water (resistivity 18.2 MΩ cm) and all the chemicals were used without further purification. The electrochemical measurements were conducted at 295 ± 2K under standard atmospheric pressure.

## 3.2 Electrode Preparation

A simple and accurate drop-coating method was employed to apply the precursor solution on a flat titanium substrate. A titanium coin (purity 99.2% basis metals, McMaster) with a dimension of 1.7×1.7×0.5 cm was used as a substrate for the Ru/Bi-oxide coatings to fabricate the electrodes.

Firstly, the titanium substrate was wet-polished using 600-grit SiC sandpaper and then rinsed and sonicated for 20 min in deionized water to remove the residues and grease. Then, the titanium substrate was put into a boiling solution of hydrochloric acid and deionized water (volume ratio of 1:1) for 20 min etching. Next, the substrate was again rinsed thoroughly with deionized water and dried under argon stream.

The Ru/Bi-oxide precursor solution of a desired composition (Ru/Bi ratio) was applied uniformly with an accurate volume of 75 μL on the newly-prepared Ti substrate using a pipet. 2 drops of the precursor solution were applied on the surface of the substrate to ensure the surface was evenly covered with the precursor solution. After applying the first coating, the substrate was placed into the furnace in air and the coating was annealed at 573.15 K for 15 min (the optimum temperature was determined by performing the procedure in the temperature range from 473.15 to 773.15 K and examining the resulting electrochemical properties in terms of the charge storage). The substrate with coating was then removed from the furnace and was placed at room temperature for cooling down

for 10 min. Then, the second layer of coating was applied. This coating procedure was repeated 5 times to form a stable $Ru_xBi_{1-x}$-oxide coating ($0 \leq x \leq 1$) coating. For the last layer, the annealing time for the substrate was set to be 60 min in order to fully oxidize the coating to form Ru/Bi-oxide composite.

## 3.3 Electrochemical Measurements

### 3.3.1 Cyclic Voltammetry

Cyclic voltammetry (CV) was performed in a three-electrode system in order to determine the electrochemical behavior of Ru/Bi-oxide coatings. A saturated calomel electrode (SCE) was used as reference electrode (RE) and a graphite rod was used as the counter electrode (CE). The graphite rod was separated by a glass frit (Ace Glass, Inc., USA) from the working electrode and reference electrode to avoid interference of potential oxygen and hydrogen evolution. A Teflon sample holder with an area of 1 $cm^2$ exposed to the electrolyte was used to accommodate the coated Ti samples which was used as a working electrode in this electrochemical cell (only one side, the coated side, of the Ti sample was exposed to the electrolyte). Argon was purged for 30 min into the 1M KOH electrolyte prior to all electrochemical tests and was continued until the end of measurements to maintain an oxygen-free environment.

In a CV measurement, the potentiostat applies an initial voltage to the working electrode (-0.8V), and then scan linearly toward the pre-set potential. The electrode potential applied to the working electrode can be expressed by Figure 5 (a). After the pre-set potential of 0.2V is reached, the voltage starts to scan reversely at the same scan rate. During the measurements, the response current of the working electrode was recorded and plotted as a function of applied voltage, Figure 5 (b). In experiments reported in the thesis, in order to compare the capacitance based on the same standard, all the potential range of CV measurements were set to be from -0.8 to 0.2 V, with a scan rate of 50 mv/s and a potential window of 1 V.

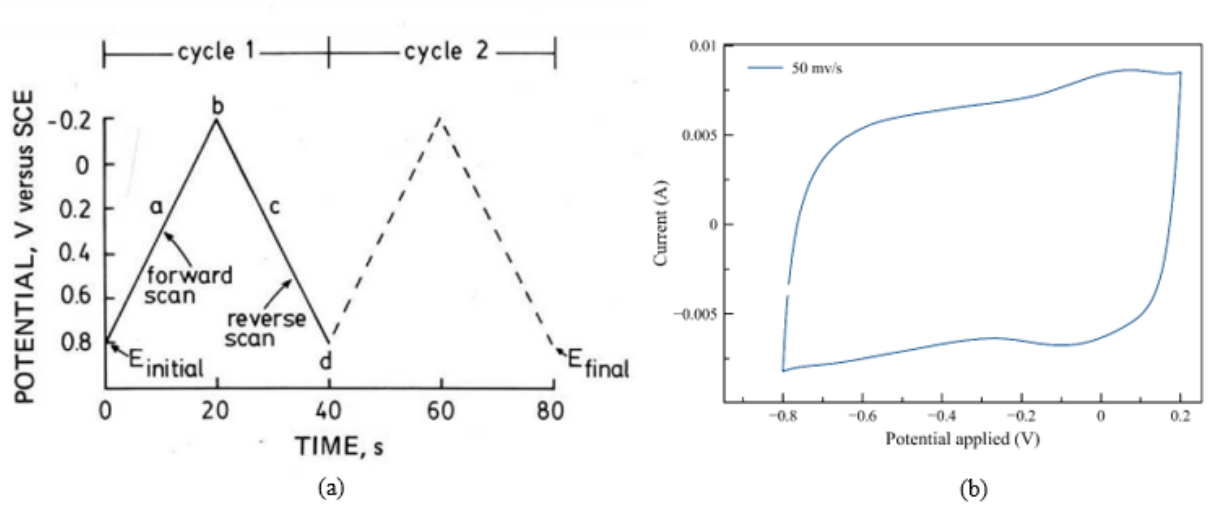


Figure 5 The potential applied on the working electrode as a function of time (a) [44] and the function of current and applied potential of working electrode in a CV test (b).

The capacitance can be calculated from the resulted CV curves using the following equation:

$$C = \frac{\int_{E1}^{E2} Idt}{\Delta V} \qquad \text{Equation 2}$$

where I is the current (A) during the CV measurement and $\Delta V$ is the pre-set potential window (V).

In order to investigate the stability of best-performing coating, GCD measurement was repeated for 3000 cycles at a scan rate of 150 mV/s to investigate the stability of the coating.

### 3.3.2 Galvanostatic Charge-Discharge (GCD)

To further understand the electrochemical properties of the materials for practical application, GCD measurements were conducted in a two-compartment cell. In this cell, two same electrodes were employed, with the Ru/Bi-oxide coated sides facing each other. In order to prevent short-circuiting and at the same time to provide electrolyte, a filter paper (Fisherbrand, 09-795B) soaked in 6M KOH was placed in between the two electrodes; this is a standard 2-electrode testing assembly for supercapacitors.

In a GCD measurement, the cell was charged from 0 V (discharged cell) to a predetermined potential (0.8V) by applying a constant current and the voltage signal was recorded as a function of time. The feature of current applied can be expressed by Figure 6 (a), respective to the 5 cycles in Figure 6 (b). For example, Figure 6 (b) represents 5 cycles of Ru-oxide coating at a current density of 3 mA/cm$^2$.

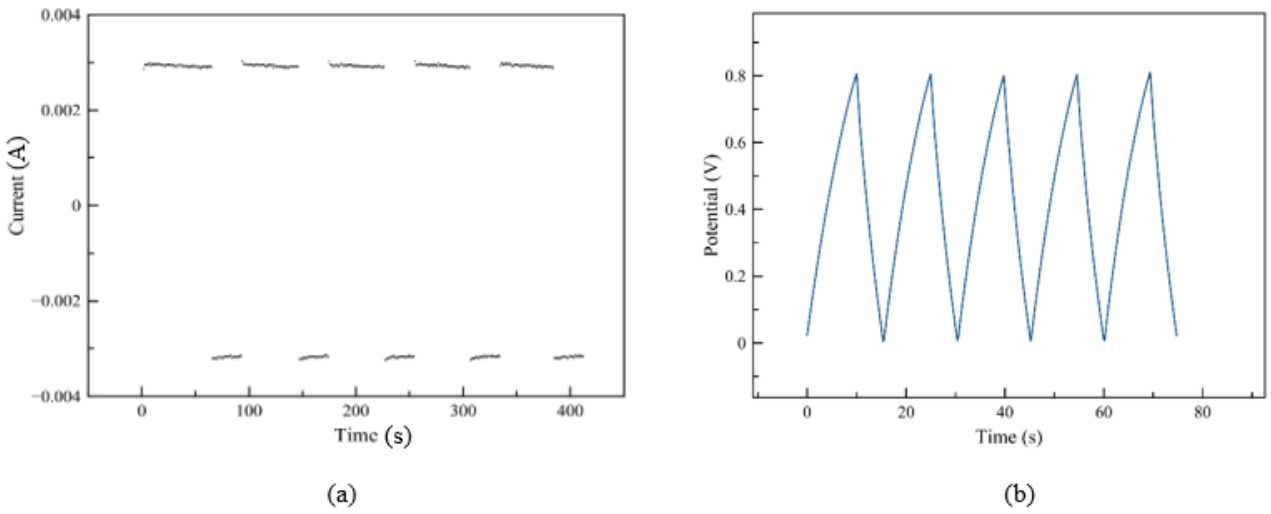


Figure 6 The current signal applied (a) and potential recorded (b) in a GCD measurement.

From the GCD measurements, many properties of the oxide coatings can be acquired, such as capacitance, cycle life, energy density, and power density.

The capacitance of the coatings can be calculated by using the equation:

$$C = \frac{I}{dV/dt} \qquad \text{Equation 3}$$

where V is the potential difference between the two electrodes (V), I is the current density applied ($A/cm^2$), C is the capacitance ($F/cm^2$), dV/dt is the slope of the GCD curve (V/s).

### 3.3.3 Electrochemical Impedance Spectroscopy (EIS)

EIS was performed in the 2-coin cell to determine the impedance of Ru/Bi-oxide coatings and interface between Ru/Bi-oxide coating and electrolyte. EIS was performed between 0.1Hz and 1MHz with an amplitude of 10 mV. Electrochemical impedance spectroscopy (EIS) measurement was further used to investigate the capacitive behavior of the Ru-oxide coatings and the electrochemical properties of the three-electrode system. In an EIS measurement, a small amplitude AC sinusoidal current signal of a certain range of frequencies is applied to the system, and the response of current is recorded. The frequency of the current can vary within a wide range from high to low frequency, which allows the separation of reactions/processes characterized by different time constants [45]. The EIS results are normally expressed graphically by Bode plot (right) and Nyquist plot (left) in Figure 7. The example is the EIS results of the pure Ru-oxide coating measured in a two-compartment cell.

Since only a small excitation signal is normally applied to the system, EIS measurement can be effectively used to evaluate the system without significantly disturbing it.

All electrochemical measurements were performed using a potentiostat (Autolab PFSTAT30, Metrohm, Netherlands) connected to a computer. All tests were carried out in room temperature and under ambient atmosphere.

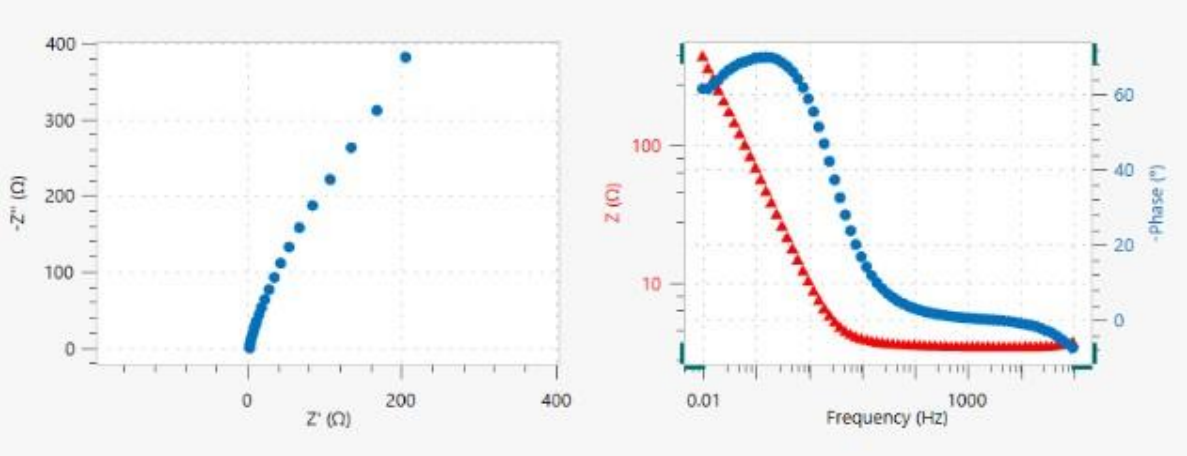


Figure 7 Example of the EIS results of the pure Ru-oxide coating measured in a two-compartment cell.

# Chapter 4: Results and Discussion

## 4.1 Effect of Annealing Temperature

The annealing temperature has a great effect on the water content of the Ru-oxide coatings and therefore to the capacitance value. According to a study by Zheng et al [46], hydrous $RuO_2$ tend to have capacitance much larger than crystalline $RuO_2$. The study shows that at temperatures below 175 °C, anhydrous $RuO_2$ peaks were observed from powered XRD patterns. From TGA measurement with a temperature scan rate of 10 °C/min, it is determined that $RuO_2 \cdot H_2O$ and $RuO_2$ were formed at a temperature of ~100 and 300 °C, respectively. The water content in $RuO_2 \cdot xH_2O$ is summarised in the flowing table as a function of annealing temperature [46].

| $T_{anneal}$ (° C) | 25 | 100 | 150 | 175 | 200 | 300 | 400 |
|---|---|---|---|---|---|---|---|
| $x(RuO_2 \cdot xH_2O)$ | 2.00 | 0.93 | 0.50 | 0.31 | 0.20 | 0.11 | 0.03 |

Table 1 Summary of the $RuO_2 \cdot xH_2O$ as a function of annealing temperature [45].

Our experiments found that the capacitance of $RuO_2 \cdot xH_2O$ is closely related to the degree of crystallinity. It was found that the coatings annealed at relatively lower temperatures can have much larger capacitance than the coatings annealed at high temperatures. However, when annealed at lower temperatures, the coatings were very unstable and easily dissolved into the electrolyte when doing the electrochemical measurements, which makes it unpractical and meaningless for real-life utilisations. It is also believed that in order to achieve larger capacitance, a compromise of electronic conductivity of the coating materials and the conductivity for protons in the hydrated pores should be reached by adjusting annealing temperatures [47]. Therefore, it is critical to determine the optimal annealing temperature that gives large capacitance and meanwhile stable enough.

In order to investigate the optimal annealing temperature of Ru-oxide with this thermal decomposition method employed in this study, a series of experiment with different annealing temperatures were initially carried out (250 °C, 275 °C, 300 °C and 325 °C).

Figure 8 shows the capacitance of pure ruthenium oxide coatings annealed at different temperatures. As we can see, at 275 °C the capacitance is maximum at 276 ± 14 $mF/cm^2$, which

exceeds results from other previous studies. However, the coatings were not stable and their dissolution in to the electrolyte was observed during electrochemical tests.

When increasing the temperature to 300 °C, there is a sudden drop in the capacitance yielding a value of 25 ± 8 mF/cm$^2$. This is believed to be caused by the formation of a large amount of crystalized $RuO_2$ which has a poor ionic conductivity and the decreased portion of $H_2O$ content in the molecule. However, unlike the coatings formed at the two lower temperatures, this coating was found to be stable. Therefore, the annealing temperature of 300 °C was set as the optimum temperature for further experiments.

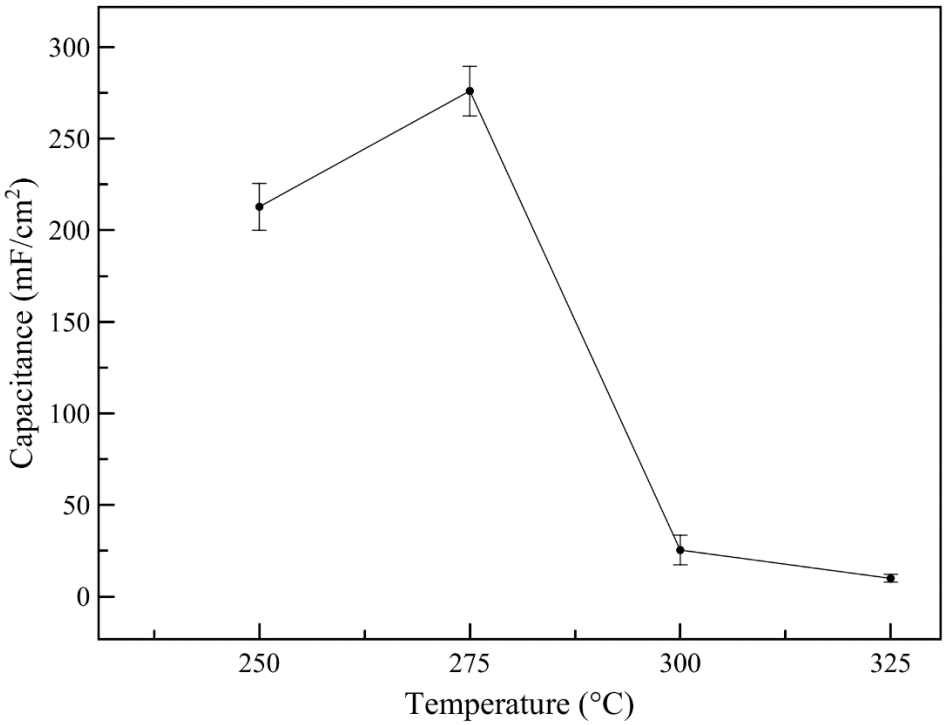


Figure 8 The capacitance of ruthenium oxides annealed at different temperatures. The data was obtained from CV experiments performed in a 3-electrode cell and with a scan rate of 50 mV/s.

## 4.2 Effect of Bi-oxide in Ru-oxide

### 4.2.1 Ruthenium Oxide Coatings

Ruthenium oxide has been favored by researchers as the most extensively studied pseudocapacitive material due to its highly reversible faradic reactions, three distinct oxidation states within a 1.2 V voltage window, high conductivity and long life cycle [12, 48, 49]. Ruthenium oxides are considered to be the best material for pseudocapacitors because its oxides have more than one valent state, which allows several redox reactions to happen at the same time and store more electrons.

The reaction mechanisms for electron storage are different depending on the electrolyte solution. When in acidic electrolyte solution, for example in $H_2SO_4$, the Ru oxidation states can change from Ru(II) to Ru(IV) accompanied by electro-adsorption of protons on the Ru-oxide coatings, which can be expressed as [50]:

$$RuO_2 + \mathrm{x}H^+ + xe^- \rightleftharpoons RuO_{2-x}(OH)_x \qquad \text{where } 0 \leq x \leq 2$$

However, it is found that when in alkaline electrolyte solutions, the $RuO_2$ will be oxidized to $RuO_4^{2-}$, $RuO_4^-$ and $RuO_4$. During the discharge process, theses high valency state compounds will be reduced back to $RuO_2$ [51].

In order to investigate the effect of adding Bi-oxide to pure Ru-oxide coatings, the 100%Ru-oxide coatings were first studied as control.

The capacitive behavior of 100%Ru-oxide coatings was first investigated in 1.0M KOH solution by cyclic voltammetry at a scan rate of 50 mV/s in a three-electrode system and the resulting CV is presented in Figure 9. The resulting capacitance was calculated to be 30 ± 4 mF/cm$^2$ by using Equation 2 from the previous chapter.

The CV curve shows almost mirror symmetry and a rectangular shape, indicating that the pure Ru-oxide coating stores charge mainly by charging the electric double-layer rather than through faradic reactions. This can explain the fact that the measured capacitance value is much smaller than the theoretical value. Nevertheless, two current “shoulders” can see seen on the CV around 0.05 V (one anodic, and one cathodic), indicating reversible redox transitions in the solid phase.

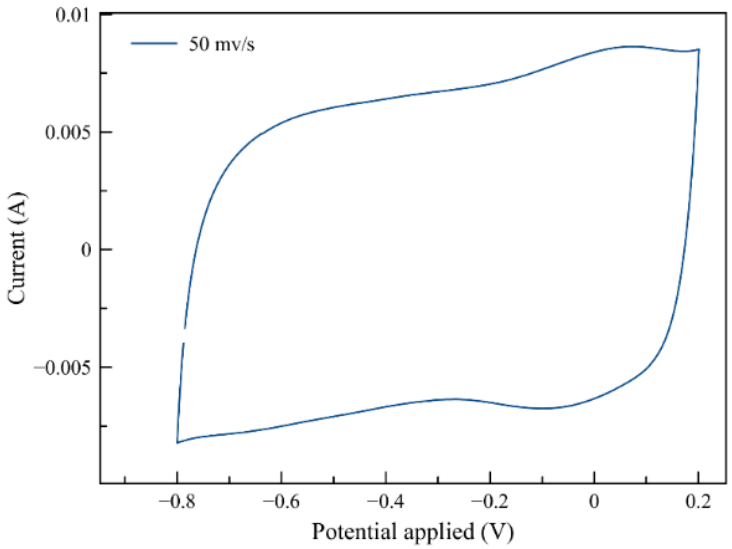


Figure 9 Cyclic voltammetry of $RuO_2$ coating at a scan rate of 50 mV/s tested in 1.0M KOH.

The pure Ru-oxide coating was also tested under different scan rates, as shown in Figure 10. From the figure, we can clearly see that with different scan rate, the current response of the working electrode varies. It is expected that with lower scan rate, higher capacitance can be achieved, as presented in Figure 10. This is most likely because at lower scan rates, the electrolyte can have sufficient time to penetrate the outer layer of the coating through pores and therefore store the charge more densely on the electrode [52]. More importantly, for pseudo-capacitance materials such as Ru-oxide, Mn-oxide and many other transition metal oxides, lower scan rate will allow enough time for the faradaic redox reactions to occur, during which the oxides react with ions from the solution ($H^+$) and contribute to the whole capacitance. Therefore, an increased capacitance of the electrode of the same material can be observed by operating at a lower the scan rate.

The electrochemical properties of pure Ru-oxide coating were further investigated by Galvanic Charge-Discharge (GCD) technique, using a two-compartment cell and 6M KOH as electrolyte. Figure 11 is the GCD plot recorded at 3 $mA/cm^2$, which shows good electrochemical reversibility and has a stable potential window of 0.8 V. By using Equation 3, the capacitance of the Ru-oxide coatings was calculated to be 24 $mF/cm^2$, which is comparable to the results acquired from CV data.

It can be noticed that the behavior of the charging process at a smaller current density of the Ru-oxide coating is not entirely linear, which suggests that the material indeed behaves as a pseudocapacitance material. In contrast, the charging and discharging pattern of an EDLC is linear.

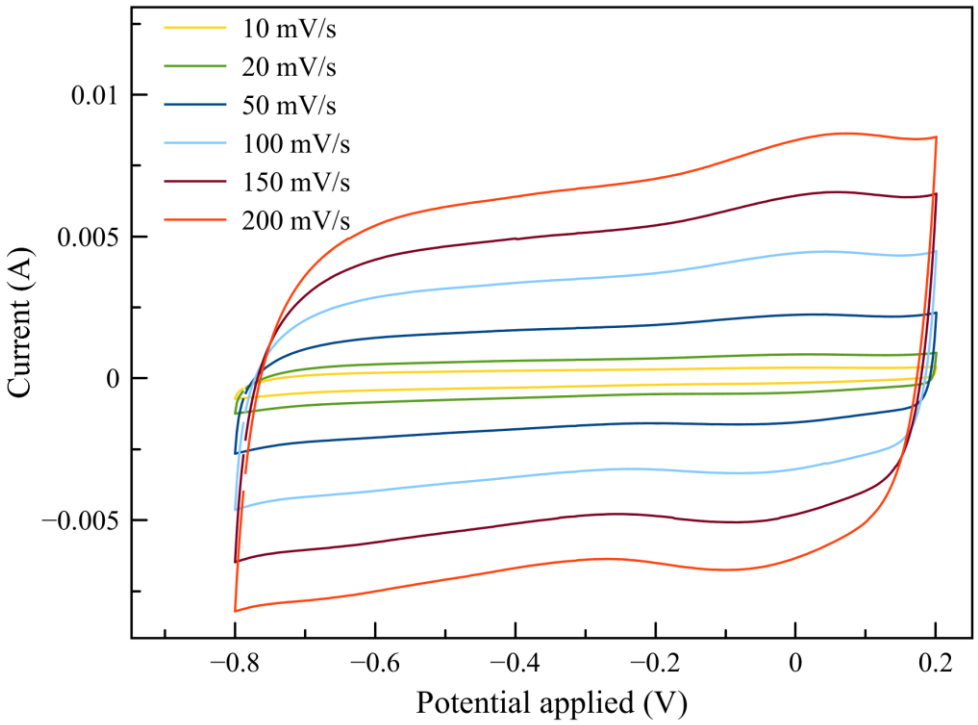


Figure 10 Pure $RuO_2$ coating fabricated at 300 °C was tested under different scan rates in 1.0M KOH.

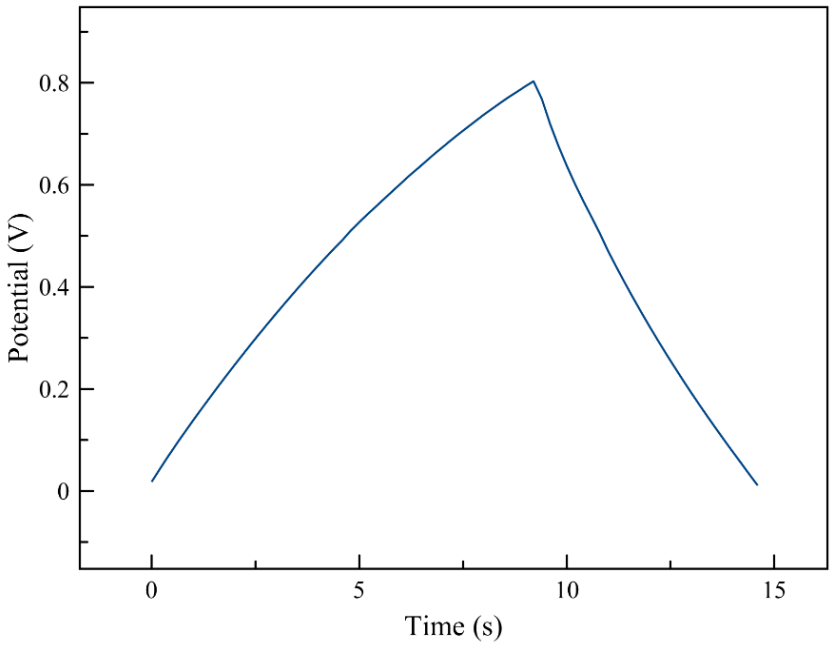


Figure 11 Galvanic charge/discharge of $RuO_2$ coating at a current density of 3 $mA/cm^2$ in 6.0M KOH.

In order to determine the equivalent-series-resistance (ESR) and behaviour of the system, EIS measurement was done. The main plot of the EIS spectra in Figure 12 indicates that there is a faradic component of the impedance, which could be evidenced by the slope of the curve. Pure capacitance material gives infinite slope, i.e. straight vertical line. This is to expect since the investigated $RuO_2$ capacitor is a pseud-capacitor, not pure double-layer capacitor. The intersection of the spectrum with the real impedance axis at high frequencies yields an ESR value of 3.5 Ω. This value represents the sum of all resistances in the system (electrolyte resistance, coating resistance, and other ohmic resistances related to the current collector and connecting leas/wires).

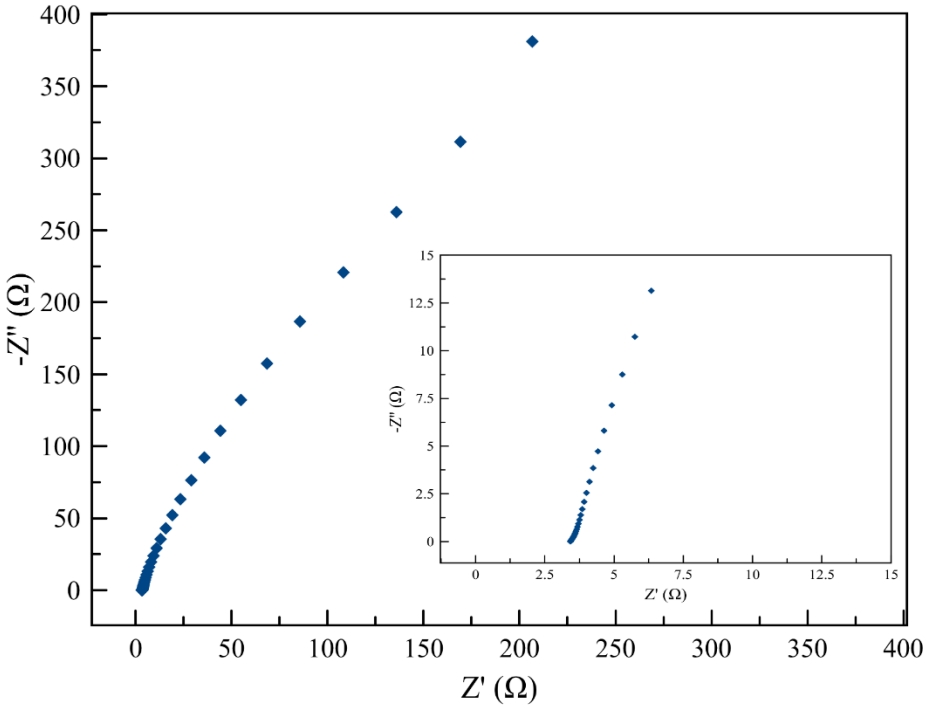


Figure 12 EIS of $RuO_2$ coating measured in a 2-coin cell at 0 V.

The surface topography and morphology of ruthenium coatings were investigated by scanning electron microscopy (SEM). It can be seen that the surface shows a cracked-mud morphology, typical for metal-oxide coatings formed on Ti employing the thermal-decomposition method. The surface does not show high porosity or other structures that can increase the surface area. From the elemental mapping, it can be noticed that the ruthenium oxides are evenly distributed throughout the surface, as shown in Figure 13.

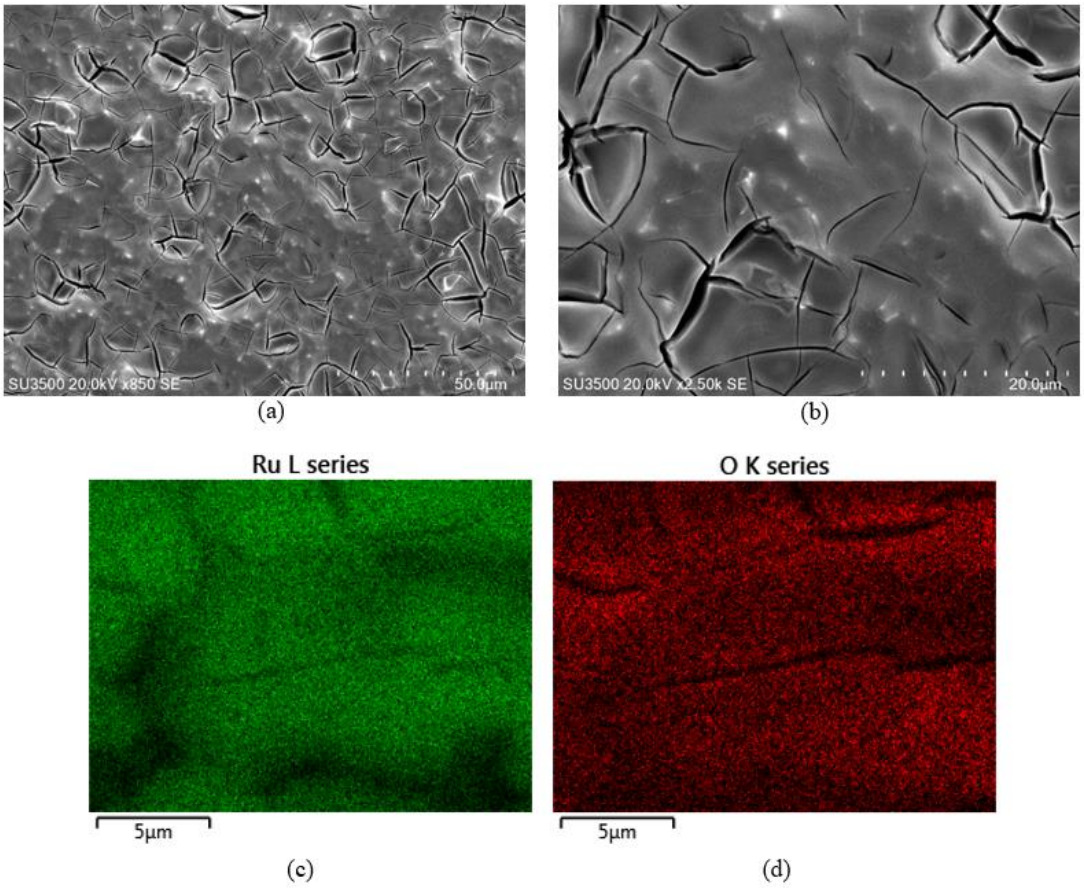


Figure 13 SEMs (a and b) and elements mappings (c and d) of Ru-oxide coatings.

### 4.2.2 Bismuth Oxide Coatings

Pure bismuth-oxide coatings were also studied by CV, GCD and EIS techniques. Bismuth oxide is also considered to be a suitable material for electrodes of supercapacitors for its excellent electrochemical properties such as dielectric permittivity, energy bandgap, and refractive index, which enabled Bi-based oxide materials suitable for a wide range of applications [53].

The 100%Bi-oxide coatings were fabricated using the same annealing method at 300 °C and were first investigated by CV in a 3-electrode system, with 1M KOH as electrolyte and a scan rate of 50 mV/s, as shown in Figure 14. Unlike with Ru-oxide (Figure 9), the behaviour of Bi-oxide is different. The CV is 'angled', indicating resistive behaviour of the coating. Also, its shape indicates that the material is not a typical and good capacitive material, under the conditions studied. Consequently, its capacitance was calculated to be 0.45 mF/cm$^2$, which is significantly lower than that yielded by pure Ru-oxide (30 ± 4 mF/cm$^2$).

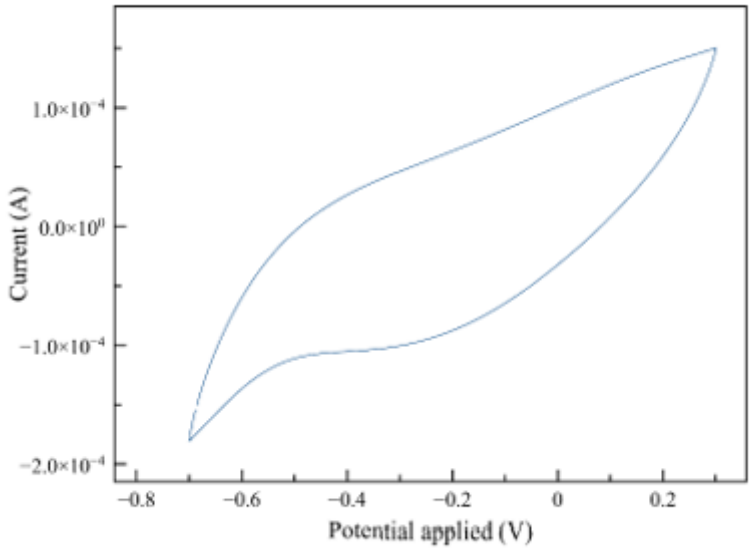


Figure 14 Cyclic voltammetry of $Bi_2O_3$ coatings with a potential window from -0.7 V to 0.3 V.

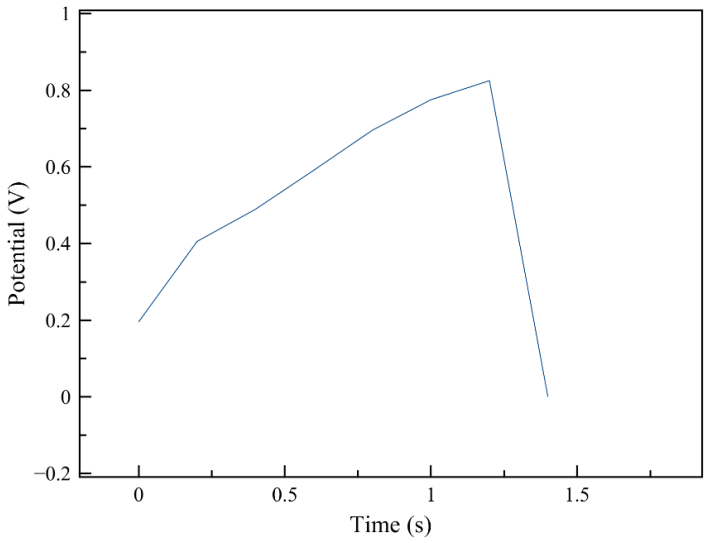


Figure 15 GCD curve of $Bi_2O_3$ at the current density of 3 mA/ $cm^2$.

The GCD was also measured in a two-compartment cell with 6 M KOH as electrolyte at a current density of 3mA/$cm^2$, as shown in Figure 15. From the GCD curve, a non-symmetrical behaviour can be observed, which indicates that the oxide is behaving as pseudocapacitive material. However, the charging and discharging curves are not similar, indicating that faradaic reactions are not reversible. From the discharge slope of the GCD, the calculated capacitance was 1.6 mF/$cm^2$.

From the SEM image of the pure Bi-oxide coatings (Figure 16), we can notice that the morphology of this oxide is quite different than that of pure Ru-oxide. The flower-like structure is uniformly distributed throughout the surface. However, from the element mapping (Figure 16 (c) and (d)) we can see that the distribution of $Bi_2O_3$ is not uniform. This surface is characterized by the presence of both Bi-oxide and Ti-oxide (not shown), the latter being formed during the coating formation procedure by dissolution of the Ti substrate.

In general, the pure Bi-oxide cannot be considered as a good candidate for supercapacitor electrodes due to its poor charge storage capacity.

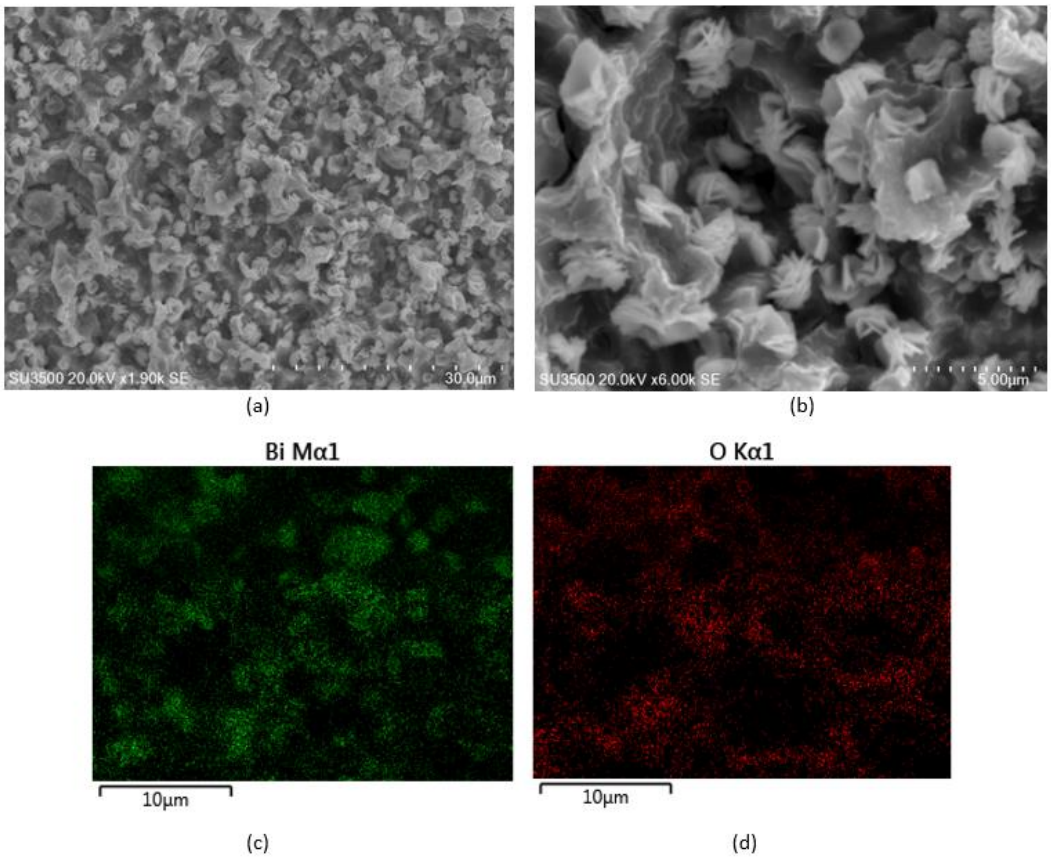


Figure 16 SEMs (a and b) and elements mappings (c and d) of $Bi_2O_3$ coatings.

### 4.2.3 $Ru_XBi_{1-x}$-Oxide Coatings

In order to produce binary Ru/Bi-oxide compositions, different ratio of Bi-oxide were added to the Ru-oxide coating by mixing the precursor solution before annealing at 300 °C in the furnace. The resulting coatings were first tested in the three-electrode cell employing CV. Figure 17 shows an example of CVs recorded on three coatings. As already mentioned, the area under the curve is proportional to the capacitance of the coating, and it can be seen that there are large differences among the three coatings. For the pure Ru-coating, a 'flat' behaviour is recorded and the capacitance (are under the curve) is smaller than on the Bi-containing Ru-oxide coatings. This gives first indication that addition of Bi into the Ru-oxide coating resulted in an increase in coating capacitance. Further, four redox-related current increases can be noticed on the two Ru/Bi-oxide coatings (two in the anodic and two in the cathodic region) indicating occurrence of reversible faradaic reactions that contribute to the charge storage. These reactions could be related to the change of oxidative states of Bi and Ru in the oxide phase.

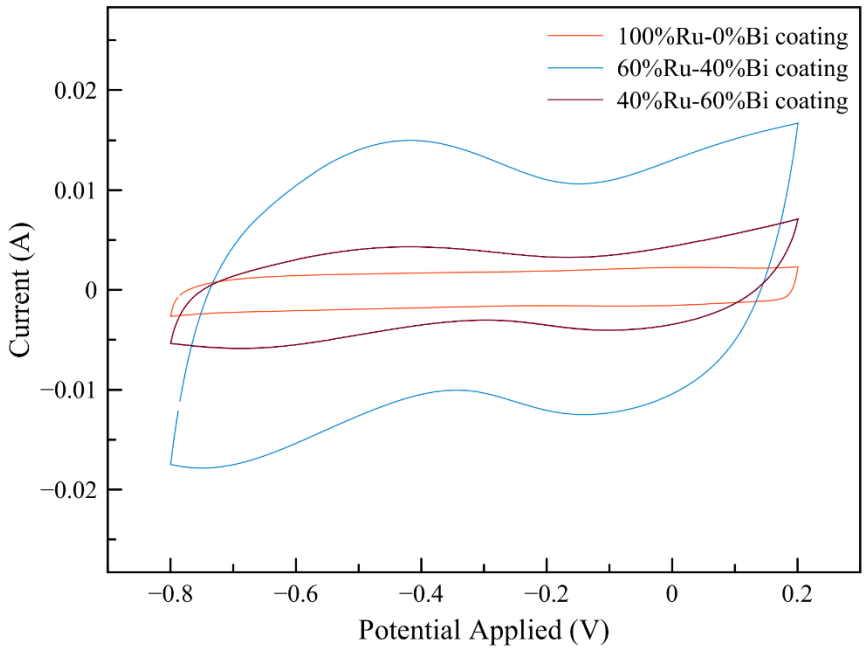


Figure 17 Comparison of CV between Ru-oxide, $Ru_{0.4}Bi_{0.6}$ -oxide coating and $Ru_{0.6}Bi_{0.4}$ -oxide coating.

From CV curves recorded on all composition, the resulting capacitance was determined and presented in Figure 18 as a function of coating composition. It was found that by adding Bi-oxide to the coating, the capacitance of the materials changed following a bell-shaped trend. The $Ru_{0.6}Bi_{0.4}$-oxide coating was found to offer the best capacitance performance; the capacitance was calculated to be 195 ± 11 mF/cm$^2$. Comparing with pure Ru-oxide material, the mixed oxide coating's capacitance increased 10-fold, which is higher than the values reported in literature [54].

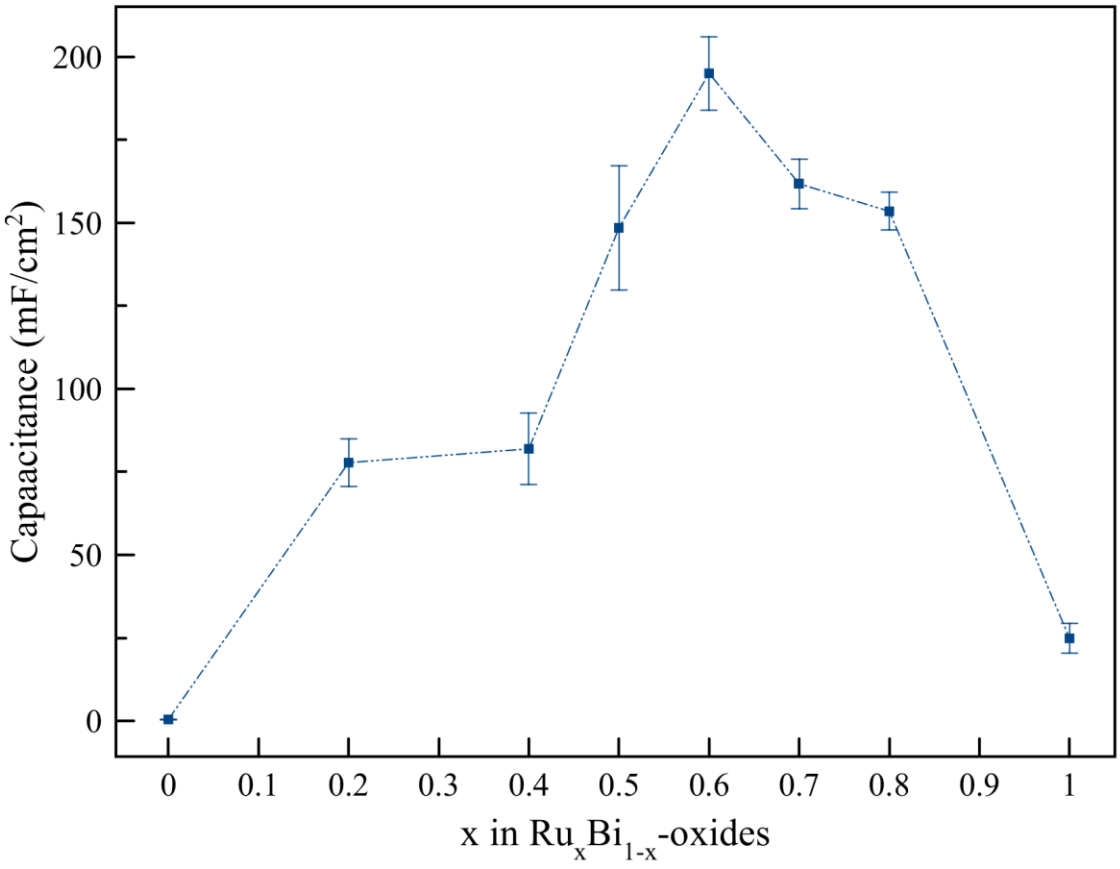


Figure 18 Capacitance of various composition of $Ru_XBi_{1-x}$-Oxide coatings calculated from CVs recorded at 50 mV/s.

In order to eliminate the effect of surface area on the capacitance, true electrochemically-active surface area (ECAS) [55] of the coatings produced in this work was determined employing a simple electrochemical method (see Appendix A.1 for details). As shown in Figure 19, the pure Bi-oxide coating is characterized by the smallest ECSA, of only 0.072 $cm^2$, which is much smaller than the actual geometric surface area of the coating exposed to the electrolyte (1 $cm^2$). This indicates that most of the Bi-oxide coating is not electrochemically active. From the figure, we can see that aside from the pure Bi-oxide coating, most of other compositions have a similar surface area of 0.626 ± 0.104 $cm^2$, with $Ru_{0.8}Bi_{0.2}$-oxide coating slightly larger (0.856 $cm^2$).

Taking into account ECSA values, capacitance values from Figure 18 were normalized to obtain the intrinsic capacitance values of the coatings and the results are presented Figure 20. As it can be seen, the maximum capacitance is still offered by the composition consisting of 60% Ru, indicating that this composition is intrinsically the best candidate for supercapacitor electrodes among the investigated coatings. It is currently not clear what origin of the differences seen in the plot is, but it could be related to the differences in structure of oxide coatings that enables different rates of $H^+$ intercalation during the charging/discharging processes, and/or to utilization of higher oxide volume for charge storage.

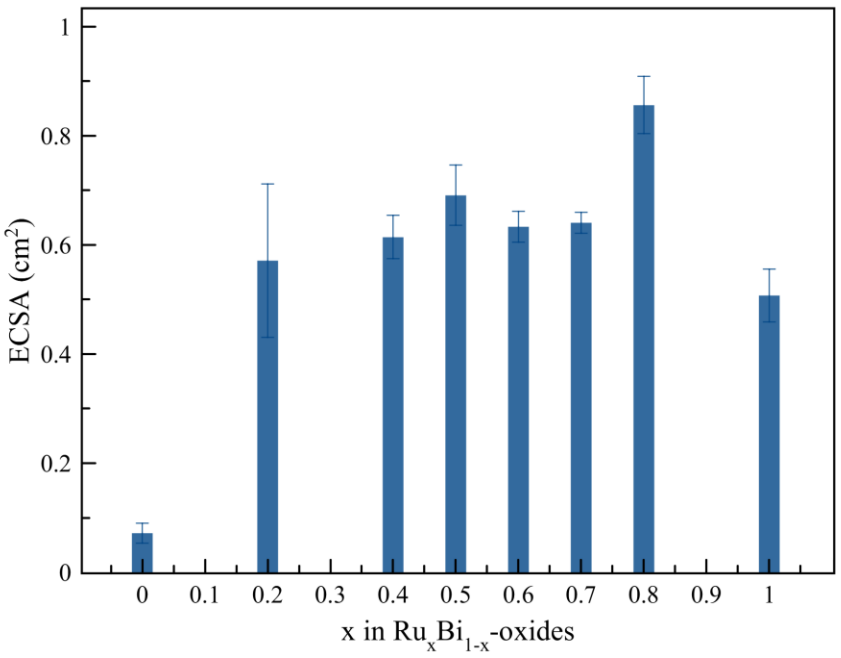


Figure 19 The ECSA of $Ru_XBi_{1-x}$-Oxide coatings.

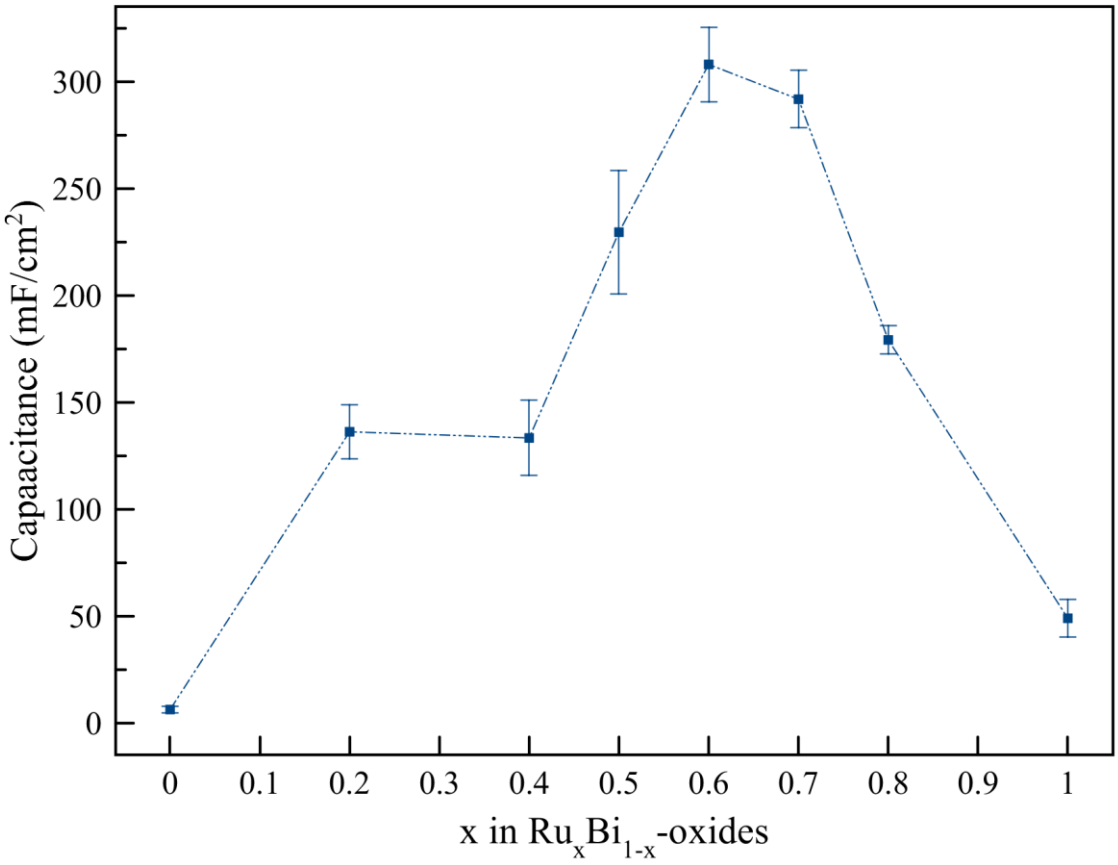


Figure 20 Capacitance of $Ru_xBi_{1-x}$ coatings after normalized by the ECAS.

Since CV measurements identified $Ru_{0.6}Bi_{0.4}$-oxide as the best-performing material, further measurements were performed only on this composition.

Figure 21 (b) shows the GCD plot recorded on the $Ru_{0.6}Bi_{0.4}$-oxide electrode in a 2-electrode cell and in 6M KOH at different current densities. In general, the shape of the GCD curve exhibited a triangular-like curve, which indicates the materials have a good electrochemical reversibility. However, at the highest current density (1 A/cm$^2$), the discharging curve is significantly different than the charging curve, indicating irreversibility of the redox reactions at this high current density.

With an increase in current density, the GCD curves shift to shorter times, indicating faster charging/discharging. At 3 mA/cm$^2$, the capacitance of $Ru_{0.6}Bi_{0.4}$-oxide was determined to be 266 ± 51 mF/cm$^2$, which is higher than the value calculated from the CV curve. However, GCD experiments

in a 2-electrode configuration are considered to replicate real charging/discharging conditions and are thus more representative than CV experiments when determining capacitance values; consequently, the above capacitance value can be taken as representative for the capacitance of $Ru_{0.6}Bi_{0.4}$-oxide at 3 mA/cm$^2$.

Figure 21 (a) shows comparison of the GCD curves of pure Ru-oxide and $Ru_{0.6}Bi_{0.4}$-oxide electrode at 3 mA/cm$^2$. The charging and discharging time of pure ruthenium oxides coating is much shorter than that of $Ru_{0.6}Bi_{0.4}$-oxide coating, suggesting that the capacitance of the later has been improved significantly by adding 40% of Bi-oxide to the pure Ru-oxide coating. Therefore, we can come to the conclusion that the addition of Bi-oxide enhanced the charge storage ability and performance of the Ru-oxide coating.

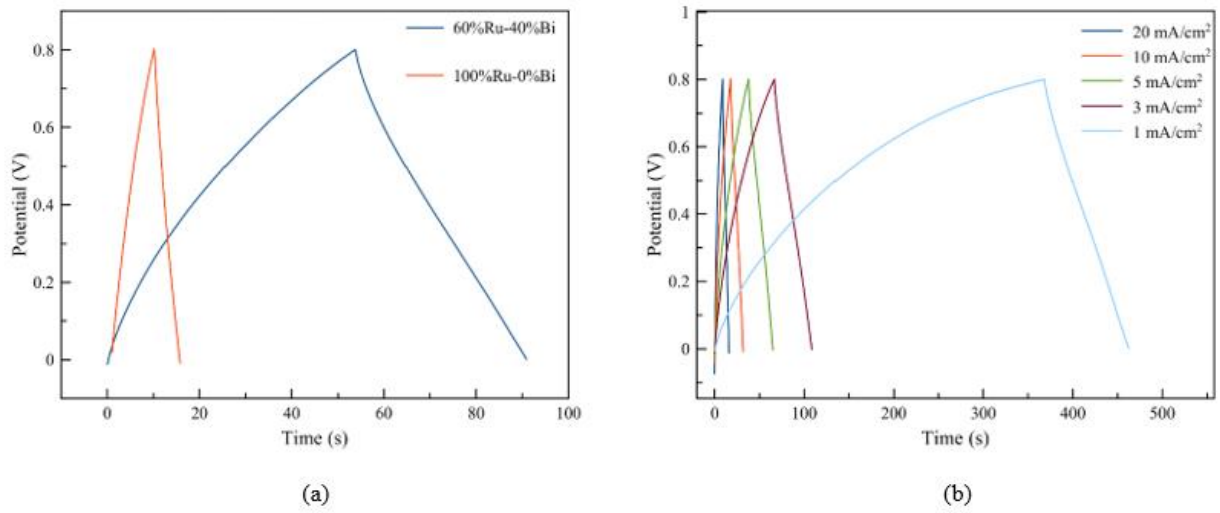


Figure 21 The comparison of GCD curves of (a) pure Ru-oxide (3 mA/cm$^2$) and $Ru_{0.6}Bi_{0.4}$-oxide and (b) GCD of $Ru_{0.6}Bi_{0.4}$-oxide coating at different current density.

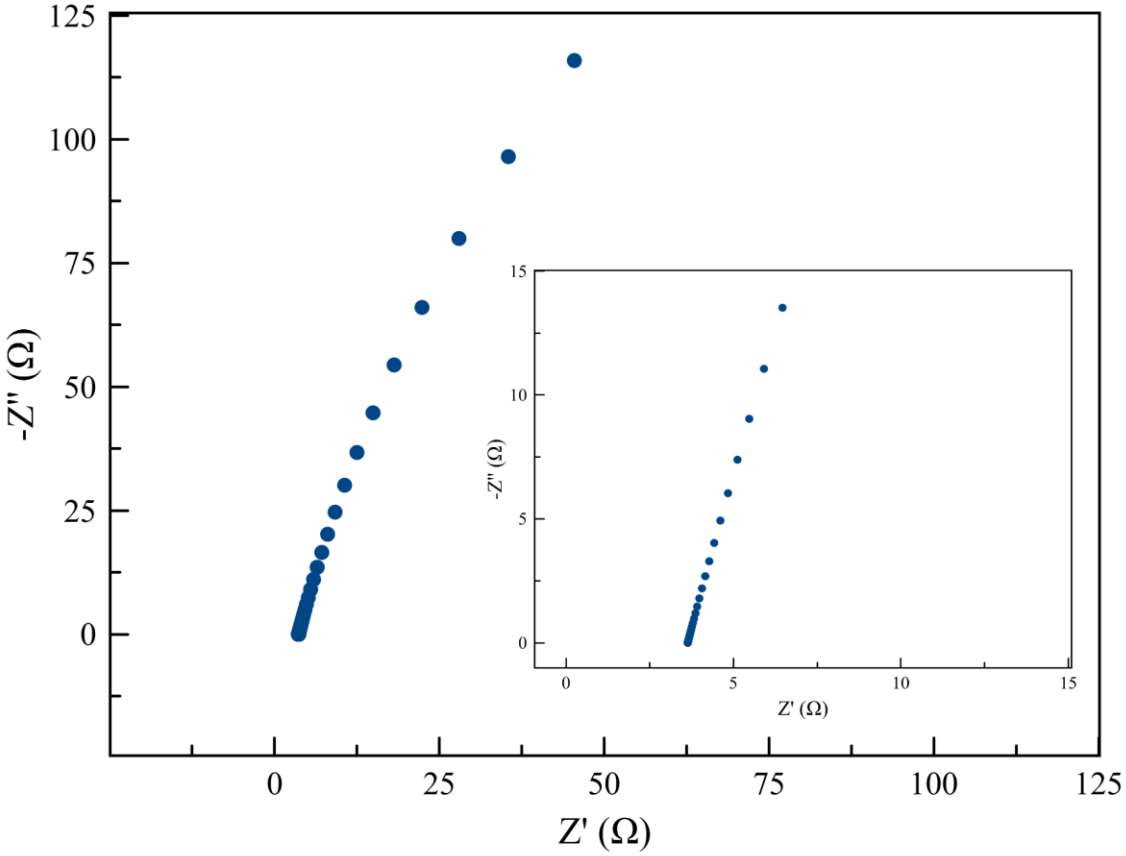


Figure 22 EIS of $Ru_{0.6}Bi_{0.4}$-oxide coating measured in a 2-coin cell at 0 V.

From the EIS of Figure 12, we can notice the faradic component of the impedance according to the slope of the curve. Similar to the EIS curve of pure $RuO_2$ coating (Figure 12), the non-vertical slope indicates the expected pseudocapacitance behaviour of the coating. The corresponding ESR value is 3.5 Ω, which is the same as the value for the $RuO_2$ coating.

One of the important properties a supercapacitor electrode material should offer is its stability. In order to test the stability of $Ru_{0.6}Bi_{0.4}$-oxide electrode, the electrode was charged/discharged over 3000 cycles employing CV at a scan rate of 100 mV/s in 1M KOH. After 3000 cycles, the capacitance reached 164.5 $mF/cm^2$, which is 86.1% of the initial capacitance. This drop is quite normal for mixed-metal-oxide coatings and can be related to structural changes in the oxide phase occurring during the charging/discharging cycle and possibly to a non-100% reversibility of redox reactions.

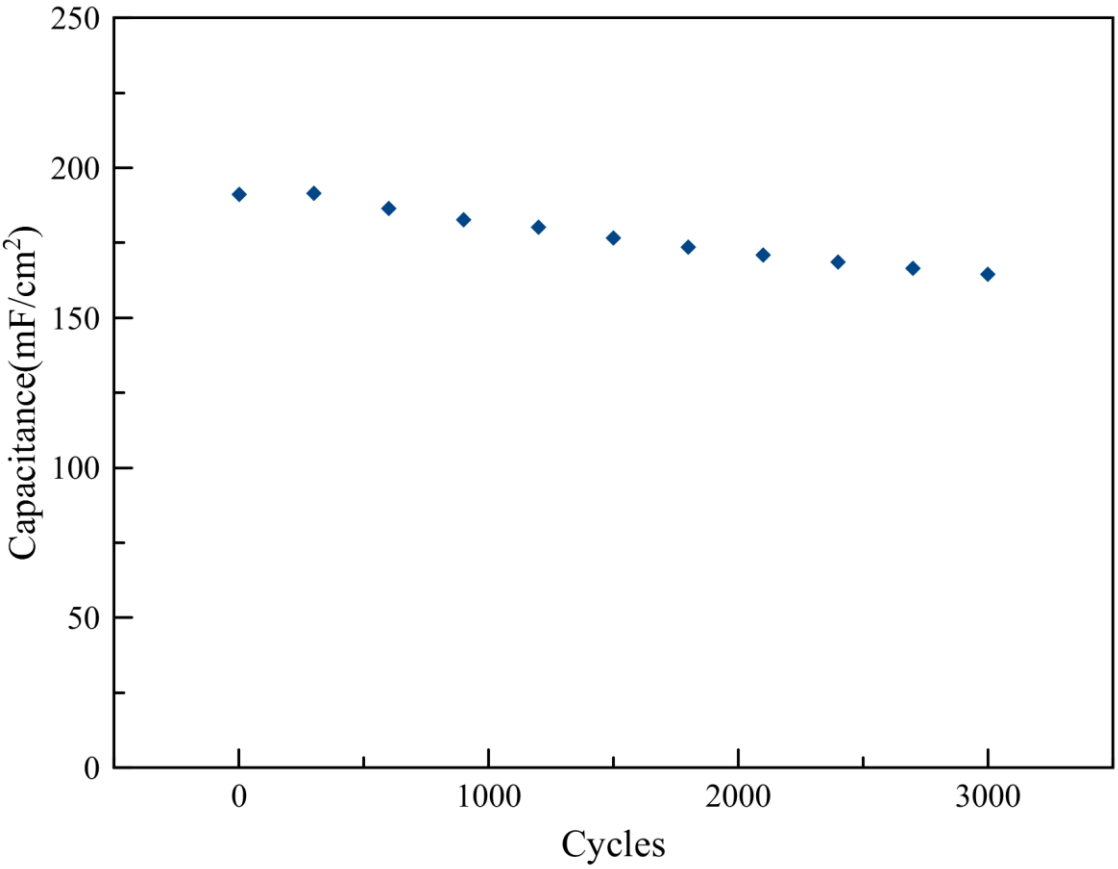


Figure 23 The stability test of $Ru_{0.6}Bi_{0.4}$-oxide electrode with 3000 GCD cycles.

The morphological analysis of the $Ru_{0.6}Bi_{0.4}$-oxide coatings was performed using scanning electron microscope (SEM). Figure 24 (a) and (b) shows the SEM image of the newly-prepared coating at two different magnifications. The image shows a uniform distribution of flower-like structures on the surface, which is beneficial for the charge storage process as it increases the contact area between the coating and the electrolyte. By comparing the SEM image of the pure ruthenium oxides coating (Figure 13) and $Ru_{0.6}Bi_{0.4}$-oxide coating, we can notice the significant difference is in the morphology of the surface. In fact, the surface morphology of $Ru_{0.6}Bi_{0.4}$-oxide coating is more similar to that of pure Bi-oxide (Figure 16) than that of pure Ru-oxide, indicating a large influence of Bi on the surface morphology.

For the commercial application of supercapacitors, this flower-like microstructure is very beneficial to increase the charge storage abilities and electrical conductivity. The structures with fine flakes will provide additional surface and interspace for cations to intercalate and deintercalate, which will benefit both the charge storage mechanism of EDLC and redox reactions and increase the overall capacitance.

Furthermore, the element mapping of the $Ru_{0.6}Bi_{0.4}$-oxide surface confirmed the uniformly distributed of Ru, Bi and O on the surface (Figure 24 (c), (d) and (e)).

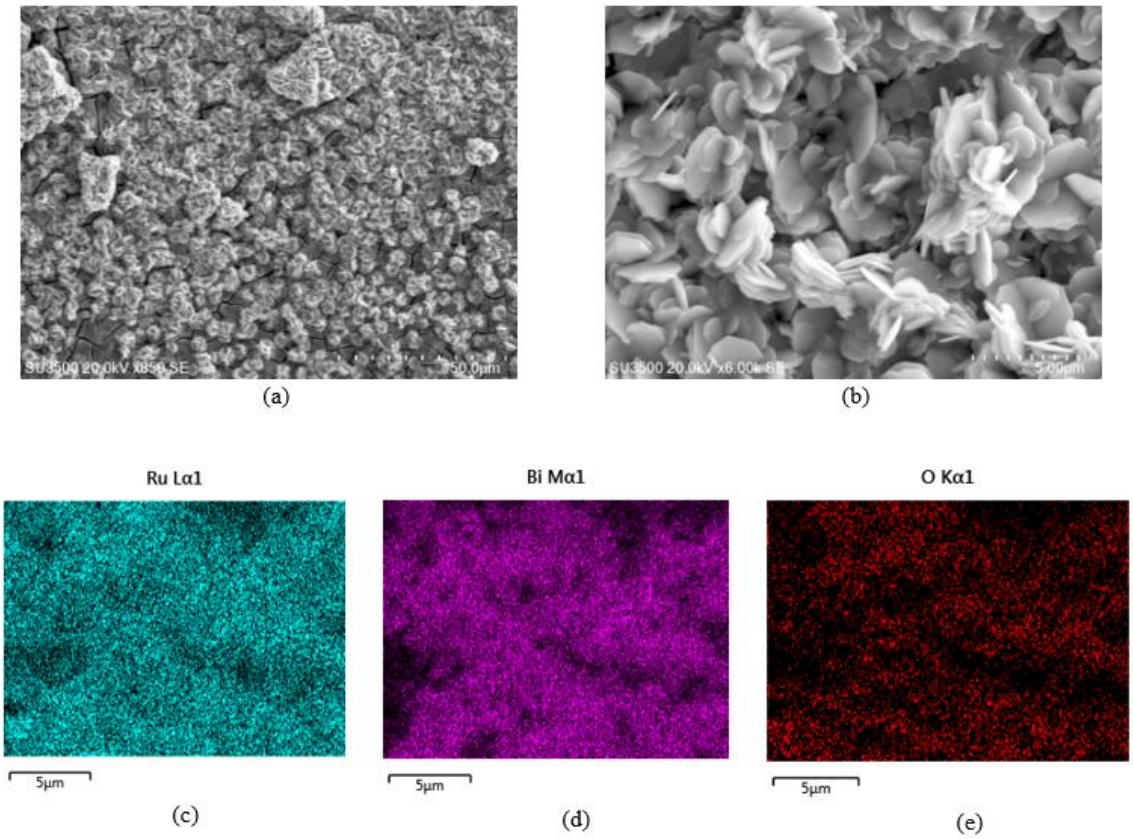


Figure 24 SEMs and element mappings of $Ru_{0.6}Bi_{0.4}$-oxide coatings.

# Chapter 5: Conclusion and Future Work

## 5.1 Conclusion

This research aimed at contributing to the development of new electrode materials for supercapacitors. Ru-oxide, as the best material for charge storage in supercapacitors, was chosen as the base material. Given its high cost, any decrease in its amount in the electrode would result in a decrease in electrode cost and bring its use closer to wide-spread application. With this in aim, we chose to add Bi into the Ru-oxide structure and to evaluate the corresponding charge storage/delivery properties of the material. Electrochemical (CV, GCD and EIS) and surface-characterization techniques (SEM/EDS) were used to investigate the properties of $Ru_xBi_{1-x}$-oxide coatings.

It was determined that addition of Bi into the Ru-oxide results in a significant change in the material's charge storage/delivery capacity. $Ru_{0.6}Bi_{0.4}$-oxide was found to offer highest capacitance ($195 \pm 11$ mF/cm$^2$ from CV measurements and $266 \pm 51$ mF/cm$^2$ from GCD measurements) with retention of 86.1% of its charge storage capacity after 3000 cycles. Comparing with pure Ru-oxide coatings ($30 \pm 4$ mF/cm$^2$) and Bi-oxides coatings (0.45 mF/cm$^2$), the $Ru_{0.6}Bi_{0.4}$-oxide coating offered a substantial increase in capacitance, i.e. by 6.5-fold comparing to Ru-oxide and 433-fold comparing to Bi-oxide. The following general conclusions resulting from this work can be acquired:

1. The annealing temperature can have a great effect on the stability and capacitance of the coatings. At temperatures higher than 275 °C, the coatings are stable, but the capacitance decreases while increasing the temperature.
2. The ratio of Ru-oxides and Bi-oxides plays an important role in determining the capacitance of the coatings. With a Ru:Bi ratio of 6:4, the capacitance of the coatings achieved the maximum value.
3. The energy density and power density of $Ru_{0.6}Bi_{0.4}$-oxide coatings as electrodes showed promising potential for pseudocapacitors applications.
4. The addition of Bi-oxide to the Ru-oxide base electrode is seen to play a major role in the structural evolution of the Ru-oxide. It is transforming the morphology of the Ru-oxide coating into a very open structure with a high surface area, providing in this way a strongly increased access to the electrolyte.

## 5.2 Future Work

A significant amount of promising research can be done focusing on mixing metal oxides with porous structural materials such as carbon black, activated carbon and graphene. Currently, we can partly conclude that the surface area is an important factor affecting the capacitance. Therefore, by combining nano-structured or large surface-to-volume ratio materials as substrates with Ru//Bi-oxides (e.g. by coating these nano-structured substrates by a thin layer of $Ru_{0.6}Bi_{0.4}$-oxide) a significant increase in overall capacitance can be achieved, resulting from both the surface area effect (substrate) and faradaic reactions in the $Ru_{0.6}Bi_{0.4}$-oxide

On the other hand, the surface area of the mixed metal oxides coatings can be enlarged by fabricating metal oxides in the form of nanoparticles. For this reason, the nano-particle sized $Ru_{0.6}Bi_{0.4}$-oxide are expected to have even larger capacitance and better electrochemical properties than the coatings presented in this research project. Several methods have already been proposed and were applied to different applications [56].

The stability tests were done for 3000 cycles; however, long term stability tests are recommended (10000+ cycles) to fully evaluate the performance of supercapacitors for real applications.

Furthermore, since ruthenium oxides are playing the major role in determining the capacitance of the coatings and are subjected to the change of annealing temperature, future research can focus on annealing coatings at lower temperatures. By adding different metal oxides other than Bi-oxides, it is possible that more stable coatings with a formula of $Ru_xM_{1-x}$-oxides (M can be transition metals such as Cu, Fe, Ir, or Ni) will be fabricated at the temperature lower than 275 °C.

# Appendix A:

## 1. The measurement of electrochemically-active area of the coatings

The true electrochemically-active area of the $Ru_{0.6}Bi_{0.4}$-oxide coatings were determined by performing CV measurements in 0.2 mM $K_3Fe(CN)_6$ in 0.1 M quiescent $KNO_3$ electrolyte (purity 99 wt%, Fisher Scientific). CVs were recorded in a range of scan rates: 1, 2, 5, 10, 12, 15, 17, 20, 25, 30 mV/s. An example of CV recorded of $Ru_{0.6}Bi_{0.4}$-oxide coating at a scan rate of 2 mV/s is shown Figure 25. The following redox reaction of the reduction of ferricyanide to ferrocyanide was used during the measurements.

$$Fe^{III}(CN)_6^{3-} + e^- \rightleftharpoons Fe^{II}(CN)_6^{4-} \qquad \text{Equation 4}$$

Then, the Randles-Sevcik equation (Equation 5) was applied to the cathodic peak. By plotting $I_p\ vs.\ v^{0.5}$, the true electrochemically-active area of the $Ru_xBi_{1-x}$-oxide coatings was calculated [57]. The results are plotted in Figure 19 in Section 4.2.3.

$$I_p = k \cdot n^{3/2} \cdot A \cdot D^{0.5} \cdot C_b \cdot v^{0.5} \qquad \text{Equation 5}$$

where k = $2.69 \times 10^5$; n is the number of moles of electrons transferred per mole of electroactive species; A is the true electrochemically-active area of the coatings ($cm^2$); D is the diffusion coefficient ($cm^2/s$); $C_b$ is the solution concentration ($mol/cm^3$); and v is the scan rate applied to the measurements (V/s).

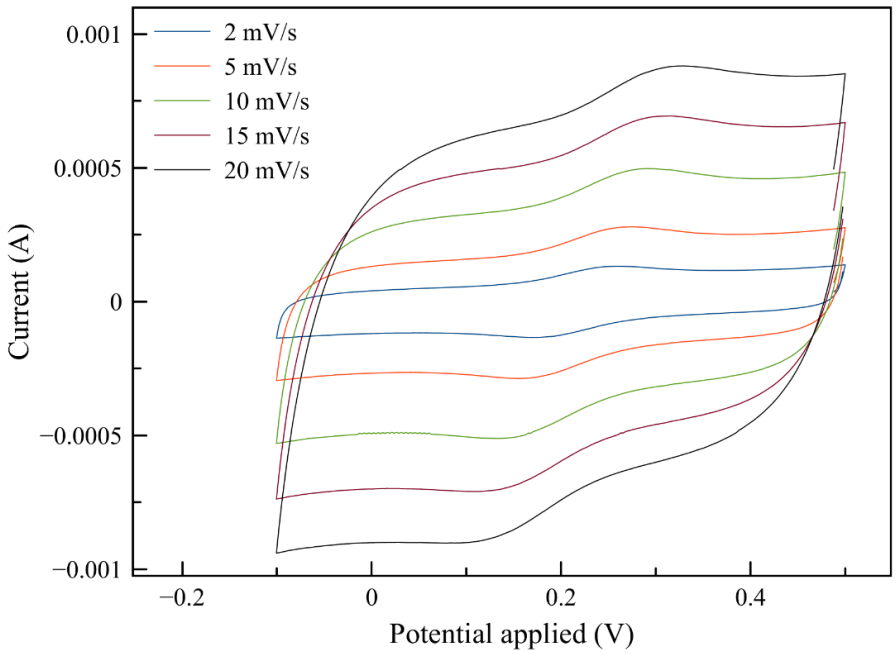


Figure 25 CV measurement of $Ru_{0.6}Bi_{0.4}$-oxide coating at a scan rate of 2, 5, 10, 15, and 20 mV/s.

# References:


[1] W.-J. Jiang *et al.*, "Understanding the high activity of Fe–N–C electrocatalysts in oxygen reduction: Fe/Fe3C nanoparticles boost the activity of Fe–N x," *Journal of the American Chemical Society*, vol. 138, no. 10, pp. 3570-3578, 2016.

[2] J. B. Cook *et al.*, "Mesoporous MoS2 as a Transition Metal Dichalcogenide Exhibiting Pseudocapacitive Li and Na-Ion Charge Storage," *Advanced Energy Materials*, vol. 6, no. 9, p. 1501937, 2016.

[3] M. Dresselhaus and I. J. N. Thomas, "Alternative energy technologies," vol. 414, no. 6861, p. 332, 2001.

[4] M. Steiner, M. Klohr, and S. Pagiela, "Energy storage system with ultracaps on board of railway vehicles," in *Power Electronics and Applications, 2007 European Conference on*, 2007, pp. 1-10: IEEE.

[5] P. Van den Bossche, F. Van Mulders, B. Verbrugge, N. Omar, H. Culcu, and H. Van Mierlo, "The Cell Versus the System: Standardization Challenges for Electricity Storage Device," in *EVS24 International Battery, Hybrid and Fuel Cell Electric Vehicle Symposium, Stavanger, Norway*, 2009.

[6] A. Namisnyk and J. Zhu, "A survey of electrochemical super-capacitor technology," in *Australian Universities Power Engineering Conference*, 2003: University of Canterbury, New Zealand.

[7] H. Wang, M. Yoshio, A. K. Thapa, and H. J. J. o. p. s. Nakamura, "From symmetric AC/AC to asymmetric AC/graphite, a progress in electrochemical capacitors," vol. 169, no. 2, pp. 375-380, 2007.

[8] Y. Honda, T. Haramoto, M. Takeshige, H. Shiozaki, T. Kitamura, and M. Ishikawa, "Aligned MWCNT sheet electrodes prepared by transfer methodology providing high-power capacitor performance," (in English), *Electrochemical and Solid State Letters*, vol. 10, no. 4, pp. A106-A110, 2007.

[9] B. Xu, F. Wu, S. Chen, C. Z. Zhang, G. P. Cao, and Y. S. Yang, "Activated carbon fiber cloths as electrodes for high performance electric double layer capacitors," (in English), *Electrochimica Acta*, vol. 52, no. 13, pp. 4595-4598, Mar 20 2007.

[10] E. Gomibuchi, T. Ichikawa, K. Kimura, S. Isobe, K. Nabeta, and H. Fujii, "Electrode properties of a double layer capacitor of nano-structured graphite produced by ball milling under a hydrogen atmosphere," (in English), *Carbon*, vol. 44, no. 5, pp. 983-988, Apr 2006.

[11] X. M. Liu *et al.*, "Impedance of carbon aerogel/activated carbon composites as electrodes of electrochemical capacitors in aprotic electrolyte," (in Chinese), *New Carbon Materials*, vol. 22, no. 2, pp. 153-158, Jun 2007.

[12] I. H. Kim and K. B. Kim, "Electrochemical characterization of hydrous ruthenium oxide thin-film electrodes for electrochemical capacitor applications," (in English), *Journal of the Electrochemical Society*, vol. 153, no. 2, pp. A383-A389, 2006.

[13] V. Augustyn, P. Simon, and B. Dunn, "Pseudocapacitive oxide materials for high-rate electrochemical energy storage," (in English), *Energy & Environmental Science*, vol. 7, no. 5, pp. 1597-1614, May 2014.

[14] A. Davies and A. P. Yu, "Material Advancements in Supercapacitors: From Activated Carbon to Carbon Nanotube and Graphene," (in English), *Canadian Journal of Chemical Engineering*, vol. 89, no. 6, pp. 1342-1357, Dec 2011.

[15] H. D. Abruna, Y. Kiya, and J. C. Henderson, "Batteries and electrochemical capacitors," (in English), *Physics Today,* vol. 61, no. 12, pp. 43-47, Dec 2008.
[16] Y. Zhang *et al.*, "Progress of electrochemical capacitor electrode materials: A review," (in English), *International Journal of Hydrogen Energy,* vol. 34, no. 11, pp. 4889-4899, Jun 2009.
[17] R. Kotz and M. Carlen, "Principles and applications of electrochemical capacitors," (in English), *Electrochimica Acta,* vol. 45, no. 15-16, pp. 2483-2498, 2000.
[18] B. E. J. C. D. Conway, University of Ottawa, "Electrochemistry Encyclopedia: Electrochemical Capacitors: Their Nature, Function, and Applications," 2003.
[19] M. S. Halper and J. C. J. M. N. G. Ellenbogen, "Supercapacitors: A brief overview," 2006.
[20] M. Jayalakshmi and K. Balasubramanian, "Simple Capacitors to Supercapacitors - An Overview," (in English), *International Journal of Electrochemical Science,* vol. 3, no. 11, pp. 1196-1217, Nov 2008.
[21] P. Simon and Y. Gogotsi, "Materials for electrochemical capacitors," in *Nanoscience And Technology: A Collection of Reviews from Nature Journals*: World Scientific, 2010, pp. 320-329.
[22] S. Stankovich *et al.*, "Graphene-based composite materials," *Nature,* vol. 442, no. 7100, pp. 282-6, Jul 20 2006.
[23] M. D. Stoller, S. Park, Y. Zhu, J. An, and R. S. Ruoff, "Graphene-based ultracapacitors," *Nano Lett,* vol. 8, no. 10, pp. 3498-502, Oct 2008.
[24] M. Moussa, M. F. El-Kady, S. Abdel-Azeim, R. B. Kaner, P. Majewski, and J. Ma, "Compact, flexible conducting polymer/graphene nanocomposites for supercapacitors of high volumetric energy density," (in English), *Composites Science and Technology,* vol. 160, pp. 50-59, May 26 2018.
[25] I. Rozenblit, "F-MWCNT/Mn/Co-oxide Electrodes for Use in High Energy-density Electrochemical Pseudocapacitors," McGill University Libraries, Doctoral dissertation, McGill University Libraries, 2015.
[26] S. W. Lee, J. Kim, S. Chen, P. T. Hammond, and Y. Shao-Horn, "Carbon nanotube/manganese oxide ultrathin film electrodes for electrochemical capacitors," *ACS Nano,* vol. 4, no. 7, pp. 3889-96, Jul 27 2010.
[27] R. A. Fisher, M. R. Watt, and W. J. Ready, "Functionalized Carbon Nanotube Supercapacitor Electrodes: A Review on Pseudocapacitive Materials," (in English), *Ecs Journal of Solid State Science and Technology,* vol. 2, no. 10, pp. M3170-M3177, 2013.
[28] K. R. Prasad and N. Miura, "Electrochemical synthesis and characterization of nanostructured tin oxide for electrochemical redox supercapacitors," (in English), *Electrochemistry Communications,* vol. 6, no. 8, pp. 849-852, Aug 2004.
[29] S. H. Park, J. Y. Kim, and K. B. J. F. C. Kim, "Pseudocapacitive Properties of Nano-structured Anhydrous Ruthenium Oxide Thin Film Prepared by Electrostatic Spray Deposition and Electrochemical Lithiation/Delithiation," *Fuel Cells,* vol. 10, no. 5, pp. 865-872, 2010.
[30] I. H. Kim, J. H. Kim, Y. H. Lee, and K. B. Kim, "Synthesis and characterization of electrochemically prepared ruthenium oxide on carbon nanotube film substrate for supercapacitor applications," (in English), *Journal of the Electrochemical Society,* vol. 152, no. 11, pp. A2170-A2178, 2005.
[31] C. C. Hu, W. C. Chen, and K. H. Chang, "How to achieve maximum utilization of hydrous ruthenium oxide for supercapacitors," (in English), *Journal of the Electrochemical Society,* vol. 151, no. 2, pp. A281-A290, Feb 2004.

[32] T. F. Hsieh, C. C. Chuang, W. J. Chen, J. H. Huang, W. T. Chen, and C. M. Shu, "Hydrous ruthenium dioxide/multi-walled carbon-nanotube/titanium electrodes for supercapacitors," (in English), *Carbon,* vol. 50, no. 5, pp. 1740-1747, Apr 2012.
[33] F. Beguin, V. Presser, A. Balducci, and E. Frackowiak, "Carbons and Electrolytes for Advanced Supercapacitors," (in English), *Advanced Materials,* vol. 26, no. 14, pp. 2219-2251, Apr 2014.
[34] X. L. Wang *et al.*, "Interlayer space regulating of NiMn layered double hydroxides for supercapacitors by controlling hydrothermal reaction time," (in English), *Electrochimica Acta,* vol. 295, pp. 1-6, Feb 1 2019.
[35] B. Dyatkin, V. Presser, M. Heon, M. R. Lukatskaya, M. Beidaghi, and Y. Gogotsi, "Development of a green supercapacitor composed entirely of environmentally friendly materials," *ChemSusChem,* vol. 6, no. 12, pp. 2269-80, Dec 2013.
[36] R. Kötz, S. Stucki, D. Scherson, D. J. J. o. e. c. Kolb, and i. electrochemistry, "In-situ identification of RuO4 as the corrosion product during oxygen evolution on ruthenium in acid media," *Journal of electroanalytical chemistry and interfacial electrochemistry,* vol. 172, no. 1-2, pp. 211-219, 1984.
[37] E. Frackowiak and F. Beguin, "Carbon materials for the electrochemical storage of energy in capacitors," (in English), *Carbon,* vol. 39, no. 6, pp. 937-950, 2001.
[38] S. J. N. N. Lee, "N. yabuuchi, BM Gallant, S. Chen, B.-S. Kim, PT Hammond, and Y. Shao-Horn," vol. 5, p. 531, 2010.
[39] Y. H. Kim and S. J. Park, "Roles of nanosized Fe3O4 on supercapacitive properties of carbon nanotubes," (in English), *Current Applied Physics,* vol. 11, no. 3, pp. 462-466, May 2011.
[40] M. A. McArthur, N. Ullah, S. Coulombe, and S. J. T. C. J. o. C. E. Omanovic, "A binder-free Ir0. 4Ru0. 6-oxide/functionalized multi-walled carbon nanotube electrode for possible applications in supercapacitors," *The Canadian Journal of Chemical Engineering,* vol. 96, no. 1, pp. 74-82, 2018.
[41] C.-C. Hu, K.-H. Chang, and C.-C. J. E. a. Wang, "Two-step hydrothermal synthesis of Ru–Sn oxide composites for electrochemical supercapacitors," *Electrochimica acta,* vol. 52, no. 13, pp. 4411-4418, 2007.
[42] K. Gopalsamy *et al.*, "Bismuth oxide nanotubes–graphene fiber-based flexible supercapacitors," vol. 6, no. 15, pp. 8595-8600, 2014.
[43] S. J. T. U. o. T. P. Lehtimäki, "Printed Supercapacitors for Energy Harvesting Applications," vol. 1463, 2017.
[44] J. Libich, J. Maca, J. Vondrak, O. Cech, and M. Sedlarikova, "Supercapacitors: Properties and applications," (in English), *Journal of Energy Storage,* vol. 17, pp. 224-227, Jun 2018.
[45] J. O. M. Bockris, B. E. Conway, and R. E. White, *Modern aspects of electrochemistry*. Springer Science & Business Media, 2012.
[46] J. P. Zheng, P. J. Cygan, and T. R. Jow, "Hydrous Ruthenium Oxide as an Electrode Material for Electrochemical Capacitors," (in English), *Journal of the Electrochemical Society,* vol. 142, no. 8, pp. 2699-2703, Aug 1995.
[47] O. Barbieri, M. Hahn, A. Foelske, and R. J. J. o. t. E. S. Kötz, "Effect of electronic resistance and water content on the performance of RuO2 for supercapacitors," *Journal of the Electrochemical Society,* vol. 153, no. 11, pp. A2049-A2054, 2006.
[48] H. Lee, M. S. Cho, I. H. Kim, J. D. Nam, and Y. Lee, "RuOx/polypyrrole nanocomposite electrode for electrochemical capacitors," (in English), *Synthetic Metals,* vol. 160, no. 9-10, pp. 1055-1059, May 2010.

[49] Q. X. Jia *et al.*, "Epitaxial growth of highly conductive RuO2 thin films on (100) Si," (in English), *Applied Physics Letters,* vol. 68, no. 8, pp. 1069-1071, Feb 19 1996.
[50] G. Wang, L. Zhang, and J. Zhang, "A review of electrode materials for electrochemical supercapacitors," *Chem Soc Rev,* vol. 41, no. 2, pp. 797-828, Jan 21 2012.
[51] Y. F. Su, F. Wu, L. Y. Bao, and Z. H. Yang, "RuO2/activated carbon composites as a positive electrode in an alkaline electrochemical capacitor," (in English), *New Carbon Materials,* vol. 22, no. 1, pp. 53-58, Mar 2007.
[52] N. Mishra, S. Shinde, R. Vishwakarma, S. Kadam, M. Sharon, and M. Sharon, "MWCNTs synthesized from waste polypropylene plastics and its application in super-capacitors," in *AIP Conference Proceedings*, 2013, vol. 1538, no. 1, pp. 228-236: AIP.
[53] T. P. Gujar, V. R. Shinde, C. D. Lokhande, R. S. Mane, and S. H. Han, "Bismuth oxide thin films prepared by chemical bath deposition (CBD) method: annealing effect," (in English), *Applied Surface Science,* vol. 250, no. 1-4, pp. 161-167, Aug 31 2005.
[54] K. Brousse *et al.*, "Laser-scribed Ru organometallic complex for the preparation of RuO2 micro-supercapacitor electrodes on flexible substrate," (in English), *Electrochimica Acta,* vol. 281, pp. 816-821, Aug 10 2018.
[55] A. Davies and A. J. T. C. J. o. C. E. Yu, "Material advancements in supercapacitors: from activated carbon to carbon nanotube and graphene," vol. 89, no. 6, pp. 1342-1357, 2011.
[56] S. Laurent, S. Boutry, and R. Muller, "Metal Oxide Particles and Their Prospects for Applications," in *Iron Oxide Nanoparticles for Biomedical Applications*: Elsevier, 2018, pp. 3-42.
[57] R. G. Compton and C. E. Banks, *Understanding voltammetry*. Journal of the American Chemical Society: World Scientific, 2011.